

University of New Mexico
UNM Digital Repository

Civil Engineering ETDs

Engineering ETDs

2-9-2010

Temporal biomass density and filamentous bacteria effects on secondary settling

Patricia A. Jones

Follow this and additional works at: https://digitalrepository.unm.edu/ce_etds

Recommended Citation

Jones, Patricia A.. "Temporal biomass density and filamentous bacteria effects on secondary settling." (2010).
https://digitalrepository.unm.edu/ce_etds/81

This Thesis is brought to you for free and open access by the Engineering ETDs at UNM Digital Repository. It has been accepted for inclusion in Civil Engineering ETDs by an authorized administrator of UNM Digital Repository. For more information, please contact disc@unm.edu.

Patricia A. Jones

Candidate

Civil Engineering

Department

This thesis is approved, and it is acceptable in quality and form for publication on microfilm:

Approved by the Thesis Committee:

 _____, Chairperson

 _____

 _____

**TEMPORAL BIOMASS DENSITY AND FILAMENTOUS BACTERIA
EFFECTS ON SECONDARY SETTLING**

BY

PATRICIA A. JONES

B.A., Environmental Science, University of Virginia, 1991

THESIS

Submitted in Partial Fulfillment of the
Requirements for the Degree of

**Master of Science
Civil Engineering**

The University of New Mexico
Albuquerque, New Mexico

December, 2009

ACKNOWLEDGMENTS

I heartily acknowledge Dr. Andrew Schuler, my advisor and thesis chair, for all of the assistance he provided over the past two years. I also thank my committee members, Dr. Bruce Thomson and Dr. Kerry Howe, for their valuable recommendations pertaining to this study and assistance in my professional development. I am grateful to Cristiano Priotto and Aaron Brennan for their many hours of help. Gratitude is extended to the National Science Foundation, Grant 0348594 for the funding to pursue this research.

I am grateful to all the wastewater facility staff and operators who assisted in making data collection possible for this study.

To my brother, Tim McClelland, thank you for the many years of support. To my friends Lara Raban and Karin Harned, who gave me immeasurable support and encouragement during this process.

And finally to my husband and children Stephen, Clara, and Marcus Jones, I could not have accomplished this without your support and love.

**TEMPORAL BIOMASS DENSITY AND FILAMENTOUS BACTERIA
EFFECTS ON SECONDARY SETTLING**

BY

PATRICIA A. JONES

ABSTRACT OF THESIS

Submitted in Partial Fulfillment of the
Requirements for the Degree of

**Master of Science
Civil Engineering**

The University of New Mexico
Albuquerque, New Mexico

December, 2009

**TEMPORAL BIOMASS DENSITY AND FILAMENTOUS BACTERIA EFFECTS
ON SECONDARY SETTLING**

by

PATRICIA A. JONES

B.A., Environmental Science, University of Virginia, 1991
M.S., Civil Engineering, The University of New Mexico, 2009

ABSTRACT

The activated sludge wastewater treatment process is the most common technology used today and solids separation is a critical and often problematic component of this technology. This leads to requirements for larger clarifiers, increased pumping costs of the diluted settled solids stream, and increased costs for solids treatment. For the past thirty years, the majority of the research in secondary settling problems has focused on the role of filamentous bacteria, and also factors such as floc size and shape. The effects of variable biomass density on settleability of biosolids produced in full scale activated sludge wastewater treatment systems has been recently been demonstrated, and seasonal variability in biomass settleability is known to occur at many wastewater treatment plants. The role of density in such temporal variations has not been previously studied.

Research evaluating temporal variation in biomass density and filamentous bacteria content and the roles these parameters play in solids separation was performed. Three different filamentous bacteria quantification methods were employed and comparison of

these methods was evaluated. Additionally, the effects of metal coagulant addition for phosphorus removal on biomass density and settleability were evaluated.

The objectives of this research were to (1) evaluate whether biomass density varies on a seasonal basis in full scale wastewater treatment systems, and if this contributes to seasonal variations in settleability, (2) evaluate if biomass density varies on a shorter timescale (weekly), and whether this is correlated with changes in settleability, (3) compare various methods of filamentous bacteria quantification, (4) investigate how precipitant addition effects biomass density and settleability.

Seasonal variation in biomass density was observed in four activated sludge plants, with high density occurring during warm weather and low density occurring during cold weather. Biomass density and filament content were both determined to influence settleability, and non-volatile solids content was strongly correlated with biomass density. Weekly variations in biomass density were not observed in selector equipped wastewater plants under stable operating conditions; however, significant variation in biomass density, settleability, and polyphosphate content were observed during process start-up and process upset events at a single full scale wastewater plant designed to perform nitrification, denitrification, and enhanced biological phosphorus removal.

Methods of quantifying filament content based on microscopic imaging were compared, including the Filament Index ranking, automated image analysis, and manual tracing methods. The filament length/floc area ratio determined by automated and manual

methods is a measure that is reliant only on information in microscope images. Filament length/dry solids were determined using a hemacytometer slide and manual tracing, which allows quantification of filaments within a known volume. The relationships between these three methods of measurements were determined, which may aid in comparisons of filament content presented in other studies, both past and future.

Precipitant addition using aluminum and iron salts was positively correlated with biomass density; however, counter to the study hypothesis, settleability degraded rather than improved. This result may be due to the development of large precipitate structures that, although of relatively high density, inhibited compaction of the biomass.

TABLE OF CONTENTS

LIST OF FIGURES	XIV
LIST OF TABLES	XIX
LIST OF ACRONYMS	XX
CHAPTER 1 INTRODUCTION.....	1
CHAPTER 2 REVIEW OF RELATED LITERATURE	4
2.1 Activated Sludge Wastewater Treatment and Settling Problems	4
2.2 Filamentous Bacteria and General Theories Explaining Bulking Sludge Causes	6
2.3 Techniques for Controlling Filamentous Bulking	7
2.4 Other Factors Contributing to Bulking Sludge	10
2.5 Seasonal Variation in Settleability	12
2.6 Quantification of filamentous bacteria.....	14
2.7 Chemical Precipitation.....	15
CHAPTER 3 RESEARCH OBJECTIVES	17
CHAPTER 4 MATERIALS AND METHODS.....	18
4.1 Sampling Methods	18
4.2 Analytical Methods.....	20
4.2.1 Suspended Solids and Phosphorus Analyses	20
4.2.2 Settleability Analysis	20
4.2.3 Density Analysis	21
4.2.4 Carbohydrate Analysis.....	22

4.2.5	Analytical Practices and Equipment	23
4.3	Filamentous Bacteria Quantification	23
4.3.1	Image Acquisition.....	23
4.3.2	Image Analysis.....	24
4.3.3	Filament Index and Filament Length per Floc Area Correlation...	25
4.4	Statistical Analysis.....	26
CHAPTER 5 SEASONAL EFFECTS ON BIOMASS DENSITY AND		
SETTLEABILITY		
27		
5.1	Introduction.....	27
5.2	Materials and methods	29
5.3	Results and discussion	30
5.3.1	Seasonal Variations.....	30
5.3.2	Density and Filament Effects on Settleability	37
5.3.3	Parameters Affecting Density.....	40
5.4	Conclusions.....	44
CHAPTER 6 DAILY CHANGES IN BIOMASS DENSITY AND		
SETTLEABILITY AT FULL-SCALE SELECTOR WASTEWATER		
TREATMENT FACILITIES.....		
46		
6.1	Introduction.....	46
6.2	Materials and Methods.....	48
6.3	Results and Discussion	49
6.3.1	Plant AX1 – March and June 2008 Sampling Events.....	49
6.3.2	Plant AN - January 2009 Sampling Event	51

6.4	Conclusions.....	53
CHAPTER 7 PROCESS START-UP AND UPSET EFFECTS ON BIOMASS		
DENSITY AND SETTLEABILITY.....		54
7.1	Introduction.....	54
7.2	Materials and Methods.....	56
7.2.1	Site Description, System Start-up and Sample Collection.....	56
7.2.2	Process Upset Event.....	57
7.2.3	Analytical Methods.....	58
7.3	Results and Discussion	58
7.3.1	System Start-up Performance	58
7.3.2	System Upset and Recovery	61
7.4	Conclusions.....	66
CHAPTER 8 COMPARISON OF IMAGE ANALYSIS METHODS FOR		
QUANTIFYING FILAMENTOUS BACTERIA.....		67
8.1	Introduction.....	67
8.2	Materials and Methods.....	69
8.2.1	Filament Index Calibration and Survey Experiment	70
8.2.2	Application of Filament Quantification Methods.....	71
8.3	Results and Discussion	72
8.3.1	Filament Index Calibration	72
8.3.2	Filament Index Study.....	73
8.3.3	Filament Data for Full Scale Wastewater Plants	76
8.4	Conclusions.....	81

CHAPTER 9 EFFECTS OF PHOSPHORUS CO-PRECIPIATION ON	
BIOMASS DENSITY AND SETTLEABILITY	84
9.1 Introduction.....	84
9.2 Materials and Methods.....	86
9.2.1 Experimental Design.....	87
9.3 Results and Discussion	90
9.3.1 Density	91
9.3.2 Settleability	94
9.3.2.1 Iron experiment effects on settleability.....	94
9.3.2.2 Aluminum experiment effects on settleability	96
9.4 Conclusions.....	98
CHAPTER 10 CONCLUSIONS.....	100
CHAPTER 10 CONCLUSIONS.....	100
CHAPTER 11 APPLICATIONS TO PRACTICE AND RECOMMENDATIONS	
FOR FUTURE RESEARCH	104
11.1 Applications to Practice	104
11.1.1 Insights to temporal variability of density and settleability at different time scales, and potential for using density measurements for process monitoring	104
11.1.2 Filament quantification methods.....	104
11.2 Recommendations for Future Research	105
11.2.1 Factors affecting seasonal density changes should be further evaluated.	105

11.2.2 Chemical precipitation effects on density and settling could be further evaluated.	106
APPENDIX A ANALYTICAL PROTOCOLS.....	107
BIBLIOGRAPHY.....	110

LIST OF FIGURES

Figure 4.1: Typical activated sludge density test results, with solution densities of 1.036, 1.039, and 1.042 g/mL, and the median biomass density value between 1.036 and 1.039 g/mL.....	22
Figure 5.1: Warm and cold weather average biomass density values for four full-scale AS plants and two MBRs.....	31
Figure 5.2: Seasonal variation of buoyant density in four AS systems. Buoyant density values are normalized to the yearly average value of each plant. “Average density” is the average of all four plants.....	32
Figure 5.3: The relationship between wastewater temperature and buoyant density in Plant AX1.....	34
Figure 5.4: The relationship between buoyant density and average ambient temperature (lagged two weeks) for the four activated sludge plants.....	34
Figure 5.5: Comparison of warm and cold weather average settling data.....	36
Figure 5.6: Non-linear regression results for empirical model (Eqn. 1) using data from all plants.....	38
Figure 5.7: Non-linear regression results for empirical model (Eqn. 1) using AS data only (MBR data omitted).....	39
Figure 5.8a: The relationship between buoyant density and NVSS/VSS for conventional AS plants.....	41
Figure 5.8b: The relationship between NVSS/VSS and Pns/VSS for conventional AS plants.....	42

Figure 5.9a: The relationship between buoyant density and NVSS/VSS for selector AS plants.	43
Figure 5.9b: The relationship between NVSS/VSS and polyphosphate content (Pns/VSS) for AS plants with anoxic (AX1 and AX2) and anaerobic (AN) selectors.	43
Figure 6.1: Daily variation in DSVI and buoyant density for the March and June 2008 sampling events at plant AX1.	50
Figure 6.2: Daily variation in soluble phosphorus content for the March and June 2008 sampling events at plant AX1.	51
Figure 6.3: Daily variation in settleability and density at plant AN (January 2009).	52
Figure 6.4: Daily variation in soluble phosphorus content at plant AN (January 2009). ...	52
Figure 7.1: Temporal changes in settleability (DSVI), buoyant density, and filament content (FL/FA) for the first six months of system operation.	59
Figure 7.2: The relationship between settleability (DSVI) and buoyant density and settleability and filament content (FL/FA) during plant start-up and stabilization....	59
Figure 7.3: The relationship between buoyant density and NVSS/VSS during system start-up and stabilization.	60
Figure 7.4: Temporal changes in settleability (DSVI), buoyant density, and filament content for the process upset and recovery event.	62
Figure 7.5 Temporal changes in buoyant density and polyphosphate during upset. The immediate change between the pre and post-upset conditions are apparent.....	63
Figure 7.6: Bar chart illustrating density, filament content, and polyphosphate pre-upset averages (Jan. 11-14), post-upset sample (Jan. 17) and post-upset averages (Jan. 18 – Feb. 12).	64

Figure 7.7: The relationship between settleability and density for pre-upset, post-upset, and the entire data set.....	65
Figure 7.8: The relationship between polyphosphate (Pns/VSS) and both buoyant density and NVSS/VSS. Pre-upset, immediately post-upset (Jan. 17), and recovery conditions are indicated.	65
Figure 8.1: The relationship between FI and FL/FA for the Jenkins et al. (2004) FI key images where the FI scale is characterized as 1: few, 2: some, 3: common, 4: very common, 5: abundant, 6: excessive. Error bars represent standard deviations of manual tracing measurements by three individuals.	73
Figure 8.2: Relationship between FI survey results and FL/FA measurements performed using automated image analysis. For comparison, the filament index calibration is included. Error bars represent standard deviations of FI ranking by 16 individuals.	74
Figure 8.3: Relationship between FI survey results and FL/FA measurements performed from manual tracing analysis. For comparison, the filament index key calibration is included. Error bars represent standard deviations of FI ranking by 16 individuals.	75
Figure 8.4: Relationship between FL/FA quantified by manual tracing (FL/FA _M) and automated (FL/FA _A) methods for images included in FI survey.....	76
Figure 8.5: Relationship between FI ranking and FL/FA measurements obtained from automated image analysis for full-scale experiment results. For comparison, the filament index key calibration is included. Error bars represent standard deviations of FI ranking by 3 individuals.....	77
Figure 8.6: Relationship between FI ranking and FL/FA measurements obtained from manual tracing of hemacytometer images for full-scale experiment results. For	

comparison, the filament index key calibration is included. Error bars represent standard deviations of FI ranking by 3 individuals.....	78
Figure 8.7: Relationship between automated and manual tracing image analysis methods for full-scale experiment results. Correlation improves and approaches a 1:1 relationship when MBR data is omitted.....	79
Figure 8.8: Relationship between FI and FL/TSS quantified from hemacytometer images using the manual tracing method. FI calibration and FL/FA _{MH} relationships are repeated here for comparison. The FL/FA units were converted from 1/μm to 1/mm to allow plotting the ratio on the same scale as the FL/TSS measurements.	80
Figure 9.1: Phosphorus removal percentage for all experiments.....	90
Figure 9.2: Relationship between buoyant density and metal dose for both iron and aluminum for phosphorus doses 50-100 mg/L.	91
Figure 9.3: Relationship between Pns content (including biomass and precipitated P) and buoyant density. Linear correlations are represented by solid lines for Fe/P and dotted lines for Al/P.	92
Figure 9.4: Relationship between buoyant density and NVSS content for iron experiments.	93
Figure 9.5: Relationship between NVSS content and buoyant for aluminum experiments.	93
Figure 9.6: Relationship between settleability (DSVI, calculated using biomass + precipitant TSS) and iron dose. Correlations are second order polynomial, and are drawn for each of the three phosphorus doses.	95

Figure 9.7: Relationship between settleability and buoyant density for iron experiments.

Correlations are second order polynomial, and are drawn for each of the three
phosphorus doses.96

Figure 9.8: Relationship between settleability (DSVI calculated using biomass +
precipitant TSS) versus aluminum dose.97

Figure 9.9: Relationship between settleability and buoyant density for alum experiments.98

LIST OF TABLES

Table 4.1 – Wastewater plant design and operating parameters.....	19
Table 8.1 – Linear regression coefficients relating filament quantification method to settleability as SVI (all correlations are positive).....	81
Table 9.1 – Experimental phosphorus and metal doses.....	89

LIST OF ACRONYMS

A/O	anaerobic/oxic wastewater treatment process
AS	activated sludge wastewater treatment
BNR	biological nutrient removal
COD	chemical oxygen demand
DO	dissolved oxygen
DSVI	dilute sludge volume index (mL/g)
EBPR	enhanced biological phosphorus removal
EPS	extracellular polymeric substance
ESS	effluent suspended solids (g/mL)
FI	filament index
FL/FA	filament length per floc area ratio (1/mm or 1/ μ m)
FL/TSS	filament length per biomass solids (m/mg)
F/M	food to microorganism ratio
HRT	hydraulic retention time
MBR	membrane bioreactor
M:D	monovalent to divalent cation ratio
NO	nitric oxide
NVSS	non-volatile suspended solids (total –volatile suspended solids, mg/L)
PAO	polyphosphate accumulating organisms
PHA	polyhydroxyalkanoates
PHB	poly-hydroxyl-butyrates
P _{ns}	non-soluble phosphorus (total phosphorus –soluble phosphorus, mg/L)
P _{sol}	soluble phosphorus (mg/L)
P _{tot}	total phosphorus (mg/L)
RAS	return activated sludge
ρ_L	liquid density (g/mL)
ρ_p	particle density (g/mL)
SM	Standard Methods
SRT	solids retention time
SVI	sludge volume index (mL/g)
TSS	total suspended solids (mg/L)
VSS	volatile suspended solids (mg/L)
WWTP	wastewater treatment plant

CHAPTER 1

INTRODUCTION

The activated sludge wastewater treatment process has advanced significantly and become more complex over the past 90 years. However, solids separation remains a critical and often problematic component of the process. Inefficient solids separation can result in diminished effluent quality, increased operations costs, increased operator oversight, and decreased treatment capacity (Parker et al., 2004). With rising energy costs, and the fact that wastewater treatment can account for up to 23% of a municipality's energy expenses (Means, 2004), the need for improved, consistent treatment performance will likely become more important with time.

The most common solids separation problem in activated sludge wastewater treatment is “bulking” sludge, where flocculated biomass fails to settle efficiently and compress adequately to keep the clarifier functioning properly. The majority of the research on solids separation problems in secondary clarifiers has focused on the role of filamentous bacteria and other factors such as floc size and shape. Excessive filamentous growth has been demonstrated to contribute to bulking conditions and numerous methods of filament quantification have been developed.

Fundamental physical principles indicate a linear relationship between a particle's buoyant density (particle density minus liquid density) and gravitational force, the driver of all settling processes. Despite this key relationship, biomass density has been largely

neglected in settling research, due to an implicit assumption that biomass density is essentially constant (Metcalf and Eddy, 2003) and possibly because indirect techniques for measuring density have yielded inconsistent results (Andreadakis, 1993).

In 1991, Dammel and Schroeder used concentration gradients of Percoll, a low osmotic pressure, high density silica solution to directly measure biomass density in full scale wastewater treatment plants (WWTPs), but they did not find correlations with settleability, possibly because of a small sample set. Schuler et al. (2001) demonstrated polyphosphate accumulation has a strong effect on density and settleability in laboratory-scale systems. Schuler and Jang (2007a) evaluated biomass density, sludge volume index (SVI), and filament content in 17 full-scale WWTP finding both density and filament content influenced SVI. They found density ranged from 1.022 to 1.056 g/mL, thus indicating that density was not constant from one plant to another, and they determined density was correlated with settleability in plants with at least moderate filament contents. They also found that non-volatile suspended solids (NVSS) content was correlated with density across all samples, and that biomass phosphorus (which includes polyphosphate) was correlated with density in plants with enhanced biological phosphorus removal (EBPR).

Previous research has found that settling performance varies seasonally at many wastewater treatment plants, with the poorest settling (highest SVI) often occurring during winter (Andreasen et al., 1996; Kruit et al., 2002, Graveleau et al., 2005).

Research by Gabb et al., (1991), Vanderhasselt et al., (1999), Parker et al., (2004), and

Pitman et al. (1983) indicated that settling performance can also vary on shorter than seasonal time scales. The role of density in such temporal variations has not been determined.

Further research relating the roles that biomass density and filamentous bacteria content play in solids separation is needed to characterize the mechanisms. In addition, variations in biomass density, both temporally (within a particular system) and spatially (across a range of treatment systems) may provide insights to improving process performance. Comparison of filamentous bacteria quantification may be useful to determine how these methods can be related to one another. Research comparing biomass density and metal coagulant addition with settleability will improve our understanding of how these parameters or additives impact settling.

CHAPTER 2

REVIEW OF RELATED LITERATURE

2.1 Activated Sludge Wastewater Treatment and Settling Problems

Municipal wastewater treatment facilities receive domestic and industrial wastewater; treat it to remove biodegradable organic matter, suspended solids, and in some cases nutrients (nitrogen and phosphorus); and discharge clarified, disinfected effluent expected to meet facility specific discharge limitations (Rittmann and McCarty, 2001). Domestic wastewater treatment is typically composed of some or all of the following unit processes: preliminary, primary, secondary, tertiary, and advanced treatment.

Preliminary treatment processes typically involve screening to remove trash and large debris, and grit removal to remove large, very rapidly-settling particulates. Primary clarification consists of settling tanks to removes additional settleable solids, including much particulate organic material, not all activated sludge WWTPs include primary clarifiers. Secondary treatment consists of biological treatment, most typically activated sludge, to remove biodegradable organic matter and secondary clarification. Secondary treatment may also include nutrient removal and disinfection. Tertiary treatment involves additional removal of suspended solids, as by granular filtration, and/or post-biological nutrient removal. Advanced treatment using advanced technologies to produce the highest quality effluent may be performed when effluent limits are stringent and/or is

intended for water reuse applications, as by membrane filtration (Metcalf and Eddy, 2003).

Since the widespread use of activated sludge began in the 1930s, secondary settling problems including bulking sludge have been commonly observed (Albertson, 1987). It is widely accepted that an excess of filamentous organisms is the primary cause of settling problems. As a result, most research concerning the control of bulking sludge has been focused on controlling filamentous growth. While this research has advanced the understanding of filamentous bacteria, it has not produced consistent control mechanisms to prevent bulking sludge (Kruit et al., 2002, Martins et al., 2004a). Control mechanisms such as selector technology were engineered to limit filamentous growth and improve settling; however, applications of selectors have been inconsistent in reducing bulking sludge events (Kruit et al., 2002, Martins et al., 2004b).

Several physical parameters of activated sludge flocs also have been researched in attempts to characterize mechanisms that may play a role in sludge settleability.

Research evaluating particle surface charge, shape, size, and extracellular polymeric substances (EPS), and floc-forming ability has been considered (Andreadakis, 1993; Liao et al., 2001; Liao et al., 2006, Jin et al., 2003, Wilen et al., 2008). Biomass density (mass per biomass volume) is the driving force in unhindered settling; however, only limited study has been devoted to evaluating this physical parameter (Schuler et al., 2001, Jang and Schuler, 2007, Schuler and Jang, 2007a,b).

2.2 *Filamentous Bacteria and General Theories Explaining Bulking Sludge Causes*

Filamentous bacteria serve both a positive and negative role in settleability. On the one hand, filaments form the backbone of sludge floc allowing floc-forming bacteria to accumulate on the filaments creating larger floc structures than might otherwise occur in the absence of filaments. On the other hand, too many filaments result in flocs that do not settle well and are resistant to compression, resulting in bulking (Metcalf and Eddy, 2003).

Substantial research has been devoted to characterizing filamentous bacteria on a morphological basis. Using identification keys developed and updated by Eikelboom (2000) and Jenkins et al. (2004), numerous researchers have identified the dominant filamentous organisms present in wastewater treatment systems worldwide. These organisms most commonly include *Microthrix parvicella*, Types 0092, and 0041/0675, and to a lesser extent *Nostocoida limicola*, *Sphaerotilus natans*, *Thiothrix* sp., Types 1851, and 021N (Martins et al., 2004a). With the advance of molecular analyses, evaluation of the physiology of specific filamentous organisms has revealed that morphologically similar filaments can have varying metabolic processes and/or vary their metabolism with the environmental conditions present (Martins et al., 2004a).

A recent review (Martins et al., 2004a) describes four general theories to explain bulking sludge. These include diffusion-based selection, kinetic selection, storage selection, and the nitric oxide (NO) hypothesis. Diffusion-based selection theory states that under low substrate conditions filamentous bacteria have a competitive advantage over floc forming

bacteria because of their high surface area to volume ratio. Kinetic selection theory maintains that filamentous bacteria are slow-growing and therefore less competitive than floc formers at high substrate concentrations. Storage selection theory holds that floc forming bacteria are better able to generate storage products (polyphosphate, glycogen, etc.) and therefore have a competitive advantage in dynamic systems where growth conditions change quickly. The NO hypothesis applies to biological nutrient removal (BNR) systems and proposes that floc forming bacteria accumulate NO as an intermediate compound during denitrification, which inhibits growth, and that filamentous bacteria do not.

Each of these theories assumes broad characteristics for either filamentous or floc forming bacteria that in many cases have not been confirmed (Martins et al., 2004a). Further, kinetic selection, storage selection, and NO hypothesis theories are each relevant for specific types of activated sludge processes and do not necessarily apply to all systems.

2.3 Techniques for Controlling Filamentous Bulking

Techniques for controlling bulking sludge fall into two categories: non-specific and specific (Martins et al., 2004a). Non-specific methods are usually applied for a limited time to control bulking. These include using oxidants such as chlorine, ozone or hydrogen peroxide to decrease the filament population, increasing sludge recycle and/or wasting rates to control the level of the sludge blanket in the clarifier, and adding cationic

polymer or talc to temporarily improve settling. While these methods can be effective, they offer only short-term control of the bulking event, because in most cases once the control measure ceases the bulking event recurs (Metcalf and Eddy, 2003). Further, non-specific methods can be costly due to increased chemical use, return sludge pumping rates and operator oversight. Specific control methods include using selectors at the beginning of the treatment process to change the substrate application to provide competitive advantage to floc-forming bacteria over filamentous bacteria. Selectors are operated in many different configurations and are discussed in more detail below.

Early research into controlling bulking sludge was conducted by Wellington Donaldson in the 1930s, who observed that plug-flow reactors resulted in more stable treatment performance (Albertson, 1987). These observations were confirmed by research conducted by Chudoba, et al. (1973), however plug-flow reactors did not become commonly incorporated into wastewater treatment design until the late 1970s. The first selector research was conducted in the 1950s by Alex Davidson. He demonstrated that combining return activated sludge and influent in an anaerobic reactor with a detention time of hours followed by aerobic treatment significantly reduced the occurrence of bulking events. According to Albertson, Davidson's research was largely disregarded until 1974 when Heide and Pasveer published studies that led to the development of the Anaerobic/Oxic (A/O) process. With the development of BNR systems in the 1980s selector technology was put into common practice.

Selectors may be separated into two categories (Metcalf and Eddy, 2003). Kinetic-based selectors include aerobic reactors at the upstream end of the biological treatment train that introduce high food to microorganism (F/M) ratios, which favor the growth of floc-forming bacteria. Kinetic selector technology assumes that floc bacteria grow faster than filamentous bacteria under high substrate conditions. Metabolic-based selectors create anoxic (containing nitrate but not oxygen) or anaerobic (containing neither nitrate nor oxygen) conditions that also have F/M ratios, but have little or no dissolved oxygen (DO) present in order to favor growth of floc-forming bacteria. Metabolic selectors rely on the assumption that floc bacteria utilize storage products (polyphosphate, glycogen, etc.) and/or are able to denitrify, while filamentous bacteria do not.

EBPR treatment systems include upstream anaerobic selectors, and they have been linked to filament control (Fainsod et al., 1999). Schuler et al. (2001) demonstrated that increased polyphosphate accumulation in bench scale EBPR systems resulted in increased biomass density and improved settleability. Concurrently, systems with separate plug-flow anoxic and/or anaerobic selectors also tended to demonstrate improved settling performance generally attributed decreased filaments (Andreasen et al., 1996, Kruit et al., 2002, Parker et al., 2004). Studies have also demonstrated that some phosphorus removal can be achieved with the use of anoxic selectors (Lugowski et al., 2007). However, not all systems with selectors experience improved settling. Some studies have documented significant and/or persistent bulking events with BNR systems designed to perform nitrification and denitrification (Andreasen et al., 1996, Kruit et al., 2002).

In a 2002 study of four full-scale WWTP, Davoli et al. found that systems with greater concentrations of soluble chemical oxygen demand (COD) in the selector effluent had reduced settleability, indicating that inadequate selector design could be a cause of poor selector performance. In a bench scale study, Martins et al. (2004b) demonstrated that microaerophilic conditions were introduced to anoxic and anaerobic reactors through turbulent mixing of influent and transport across the gas-liquid surface with sufficient oxygen introduction to negatively impact treatment performance. Therefore, the observed performance problems with some selectors might largely relate to design and operation issues rather than inherent problems with the principles involved.

2.4 Other Factors Contributing to Bulking Sludge

Activated sludge physical parameters such as particle surface charge, shape, size, extracellular polymeric substances (EPS), and floc forming abilities have also been researched in an attempt to characterize mechanisms that may play a role in sludge settleability. Andreadakis (1993) evaluated floc size, density, specific surface area, settleability (by SVI), EPS, and carbohydrate content of seven bench scale activated sludge units. The results demonstrated a correlation between floc size and density, with density increasing as floc size decreased, a correlation between SVI and specific surface area, and no correlation between carbohydrate content and SVI. The biomass density was reported in this study as 1.015 to 1.034 g/cm³, but this was by an indirect method relying on interference microscopy. Liao et al. (2001) found that EPS had a negative

effect on sludge compressibility but little effect on flocculation. Jin et al. (2003) found that floc size, fractal dimension, and filament index (FI) were strongly correlated to SVI with small, compact, low FI flocs having lower SVI. Liao (2006) found that solids retention time (SRT) did not correlate to median floc size; however, SRT did correlate to effluent suspended solids (ESS) concentration with longer SRT resulting in lower ESS.

Activated sludge biomass density measurement has been largely neglected in evaluating parameters that influence settleability. However, as demonstrated by well-established

settling models, including Stokes $\left(v = \frac{d^2(\rho_P - \rho_L)g}{18\mu} \right)$ and Cho et al. (1993),

$\left(v = \frac{\varepsilon^4(\rho_P - \rho_L)g}{(1 - \varepsilon)K\mu' a^2} \right)$, buoyant density, defined for the purposes of this research as the

particle density (ρ_p) minus the liquid density (ρ_L), is the driving force for settling.

However density has been largely neglected in previous research. One reason for this is that until recently, it was generally assumed that activated sludge biomass density was essentially constant. For example, common references such as Metcalf and Eddy (2003), report a single value (1.005 g/mL) for activated sludge density. Second, most methods used in measuring biomass density such as interference microscopy and dry solids/bound water content have been difficult to employ and the results have been highly variable (Andreadakis, 1993). Other methods have involved using Stokes-like relationships and measurements of settling velocity, floc size and shape, etc. to calculate biomass density, but the results from these methods are also highly variable.

The assumption that biomass density is constant has been refuted by bench and full-scale research. Dammel and Schroeder (1991) were the first to directly measure activated sludge density using a gradient solution of Percoll, a high density and low osmotic pressure solution of silica particles. Using a modified version of a method developed by Dammel and Schroeder, Schuler and Jang found biomass density values ranged from 1.02 to 1.056 g/mL in 17 full-scale WWTF (2007a). In particular, it was demonstrated that polyphosphate content, induced by the EBPR process, and SRT were positively correlated with density.

2.5 *Seasonal Variation in Settleability*

Seasonal variations in settling performance across a range of biological wastewater treatment technologies including conventional activated sludge, activated sludge systems with selectors, nitrification/denitrification systems, EBPR, and membrane bioreactors (MBR) have been observed (Andreasen et al., 1996; Kruit et al., 2002; Gravaleau et al., 2005, Al-Halbouni et al., 2007). In general, poorer settling performance (as indicated by higher sludge volume index, or SVI values) has been reported during winter months, while improved settling has been reported during the summer. Specifically, Kruit et al. (2002) indicated an apparent seasonal pattern in 4 plants performing EBPR and nitrification/denitrification, with higher SVI values in the winter and spring and lower values in summer.

Andreasen et al. (1996) surveyed SVI values at approximately 100 Danish wastewater plants and found SVI values were on average higher in winter than summer in the total data set, and also in EBPR and non-EBPR plant subsets. Filament content showed little variation. Graveleau et al. (2005) reported similar trends in settling data from 964 wastewater plants in France with average SVI values of 171 and 145 mL/g in the winter and summer, respectively. Wilen et al. (2008) conducted a two year study at a single full-scale wastewater plant performing nitrogen removal using pre-denitrification and post-nitrification in a trickling filter and phosphorus removal through precipitation in the primary clarifier. This study concluded that there was no seasonal difference in settleability. These research results demonstrate that seasonal differences in settleability are common but do not occur in all full-scale plants.

Other studies have suggested that settleability may be variable on a shorter time scale, such as weekly or even daily, but have not specifically evaluated this possibility. In a survey of activated sludge plants in South Africa, Gabb et al. (1991) found that settling characteristics could change rapidly (within one month) suggesting temporal variability on time scales shorter than seasonal. Vanderhasselt et al. (1997) found that changing lab scale process parameters, such as aeration intensity, could change settleability over the course of hours. A study of 21 activated sludge plants with anaerobic or anoxic selectors found that SVI could vary significantly over the course of days (Parker et al., 2004). Empirical evidence from full-scale plants demonstrated that cyclic changes in EBPR performance can impact settleability (Pitman et al., 1983) and lab scale research demonstrated that decreased influent flow characteristic of weekend conditions without

corresponding adjustment in aeration can result in depletion of poly-hydroxyl-butyrate (PHB) which in turn diminishes EBPR performance (Brdjanovic et al., 1998, Lopez and Morgenroth, 2003). Further, both external (introduction of toxics, wet weather high flow, etc.) and internal (filamentous bulking, equipment failure, etc.) system disturbances can cause process upset and quickly result in ineffective organics removal, ineffective nitrification, deflocculation (increased effluent solids), and non-filamentous foaming (Metcalf and Eddy, 2003, Love and Bott, 2000)..

Since biomass density is a fundamental driving force in settling and excess filamentous bacteria content is a known factor inhibiting settling, further research into the possible seasonal nature of these parameters is warranted. Noutsopoulos et al. (2007) observed a seasonal difference in the type of filamentous bacteria present in 17 full-scale activated sludge plants in Greece with *M. parvicella* dominant during winter and Type 0092 dominant during summer. The Graveleau et al. (2005) study also evaluated type and prevalence of filamentous bacteria and found no significant seasonal difference.

2.6 *Quantification of filamentous bacteria*

Until recently, quantifying filamentous growth has most commonly been performed through visual inspection techniques which rank relative quantities of filaments, a procedure developed by Jenkins et al. (2004). Although this method is quick and effective if performed by a trained observer, it may be criticized for its basic subjective evaluation. With the advance of digital photography used in conjunction with phase

contrast microscopy, several researchers have developed computer based image analysis tools that allow quantification of the filament and aggregated floc content (Amaral et al., 2002, Amaral and Ferreira, 2005, Banadda, et al., 2005, da Motta et al., 2002, , Jenne et al., 2006, Mesquita et al., 2008, and Mesquita et al., 2009). Additional quantification methods were developed using manual tracing to quantify filament length per volume to allow comparison with solids content resulting in filament length per mass measurement (Matsui and Yamamoto, 1984 and Takashima and Yamamoto-Ikemoto, 2003).

2.7 Chemical Precipitation

Chemical precipitation is commonly used at wastewater treatment plants to comply with effluent phosphorus limits. The most common precipitants used to precipitate dissolved phosphorus are iron, aluminum, and calcium (Metcalf and Eddy, 2003). Precipitant addition can be performed at various stages of a wastewater treatment train. Chemicals can be added to the influent for precipitation in the primary clarifiers thus removing phosphorus before the biological reactors, referred to as pre-precipitation. Simultaneous or co-precipitation involves adding chemical to the biological process resulting in phosphorus removal during secondary clarification. Tertiary or post-precipitation involves adding chemical to the secondary effluent and removing precipitates in a separate settling/removal process (Bratby, 2006). In many WWTPs, phosphorus removal is performed using chemical precipitants.

There is a great deal of design and operation data available that characterize optimum chemical dosing to achieve specific phosphorus removal goals (Bratby, 2006, Metcalf and Eddy, 2003). A 2006 experiment to evaluate the effects of chemical addition on biomass density demonstrated a positive correlation between precipitant and density but failed to correlate with SVI (Jang, 2006). Reported studies indicate variable changes in settling performance depending upon the metal salt used. Paris et al. (2005) and Parsons and Berry (2004) reported that aluminum salt addition (AlCl_3 or Alum) resulted in improved settling performance. Clark et al. (2000) reported that ferric salt addition resulted in consistently higher effluent solids with ferrous salt addition. In contrast, Parsons and Berry (2004) reported that ferrous salts degraded settling more than ferric salt addition. Additional research evaluating the relationships between chemical precipitation, biomass density, and settleability is warranted.

CHAPTER 3

RESEARCH OBJECTIVES

It was hypothesized that: (1) biomass density varies on a seasonal basis, and this contributes to seasonal variations in settleability, (2) weekly variation in biomass density at plants with selectors exists, and this is correlated with changes in settleability, including variations due to plant upsets, and (3) precipitant addition is positively correlated with biomass density. The bases for these hypotheses lie in previous research, discussed above.

The objectives of this research are to: (1) determine the seasonal variation in density and filaments at full-scale WWTPs, and evaluate correlations with settleability, as well as the relationships between density, NVSS and Pns, (2) determine weekly density and SVI patterns in full-scale systems, including variations during a process upset, (3) evaluate how precipitants added to remove phosphorus influence biomass density and settleability.

The approach of this project was to evaluate temporal changes in settleability at full-scale WWTPs by conducting a full year of periodic sampling, including sampling over a shorter time scale to evaluate variations during a plant upset. The effects of precipitant addition were evaluated in a bench scale project using activated sludge from a full-scale WWTP.

CHAPTER 4

MATERIALS AND METHODS

4.1 Sampling Methods

Activated sludge and secondary effluent samples were collected from five activated sludge wastewater treatment facilities. Recycle and permeate samples were also collected from two MBR facilities. Secondary effluent/permeate was used to dilute activated sludge samples when necessary to perform specific analyses. Samples were collected for 13 months at varying frequencies from six WWTPs and for 7 months from the seventh WWTP and are discussed in detail. The design and operating parameters for each of these wastewater treatment facilities is included in Table 4.1. Every effort was made to consistently sample each plant on the same day of the week in evaluating the seasonal changes thus mitigating possible influence from weekly variations. Analytical methods employed are discussed in detail below.

Table 4.1 – Wastewater plant design and operating parameters

Plant Name	Configuration	Design Flow (mgd*)	Average Daily Flow (mgd*)	SRT (days)
CAS1 (Belen)	2 parallel aerobic reactors (extended aeration), 2 secondary clarifiers, chlorine disinfection	1.2	0.8	18-30
CAS2 (Los Lunas)	2 parallel aerobic reactors, 2 secondary clarifiers, UV disinfection	1.0	1.0-1.3	6-8
AX1 (ABQ)	8 primary clarifiers, 14 anoxic-aerobic reactors, 12 secondary clarifiers, chlorine disinfection	76	60	6-9
AX2 (Rio Rancho #2)	Anoxic selector, 2 parallel aerobic reactors, 2 secondary clarifier, chlorine disinfection	3.5	3.5-4.5	5-8
AN (Bernalillo New)	Anaerobic selector, 2 parallel alternating anoxic-aerobic reactors, 2 secondary clarifiers, UV disinfection	1.2	0.7-1.0	18-40
MBR1 (Rio Del Oso)	2 parallel aerobic reactors, membrane filtration, chlorine disinfection	0.3	0.15	25+
MBR2 (Rio Rancho #6)	4 parallel aerobic reactors, membrane filtration, chlorine disinfection	0.625	0.25	30+

*mgd – million gallons per day

The following sampling collection procedures were observed. At the activated sludge facilities, approximately 1.5 liters of activated sludge were collected at the outfall from the final treatment reactor and 3 liters of secondary effluent were collected following secondary clarification, prior to disinfection. At the membrane bioreactor facilities, sludge was collected from the recycle unit and effluent was collected from the permeate

line. Samples were poured into Nalgene bottles, labeled, and placed in a cooler with ice packs for transport back to the lab.

4.2 Analytical Methods

4.2.1 Suspended Solids and Phosphorus Analyses

Total and volatile suspended solids (TSS, VSS) were analyzed by Standard Methods (SM) 2540 (D and E) and NVSS was the difference between TSS and VSS (American Public Health Association, et al., 2005). Total and soluble phosphorus were analyzed using a persulfate digestion method (SM 4500-P B.5) and the vanadomolybdophosphoric acid colorimetric method (SM 4500-P C), respectively. Non-soluble phosphorus (Pns) was calculated as the difference between total and soluble phosphorus.

4.2.2 Settleability Analysis

Dilute SVI (DSVI) was as described in Jenkins et al. (2004). Typically, 100 to 500 mL of well-stirred activated sludge or MBR sample (at approximately 22° C) was placed in a 1000 mL graduated cylinder, followed by dilution to 1000 mL with secondary effluent. The cylinder was inverted three to four times to mix, and after 30 minutes of quiescent settling the settled volume of the biomass was recorded. The DSVI was calculated as:

$$\left[\frac{\text{SettledVolume}(mL)}{(\text{StartVol}(mL)) * TSS\left(\frac{mg}{L}\right) * \frac{L}{1000mL} * \frac{g}{1000mg}} \right] = DSVI\left(\frac{mL}{g}\right)$$

4.2.3 Density Analysis

Biomass density was analyzed as described in Schuler and Jang (2007a, b). The method is described briefly. Activated sludge was added to a series of prepared solutions with incrementally increasing densities. The density solutions were prepared using Percoll (Amersham Life Sciences Inc., Arlington Heights, IL), which is a high density (1.13 g/mL), a low osmotic pressure suspension of silica particles diluted with secondary effluent. One milliliter of well-stirred activated sludge (at approximately 22°C) was added to a 1 milliliter prepared density solution in a culture tube. Due to very high solids content (7-15 g/L) at the MBR plants, these sludge samples were diluted with permeate to approximate 2-3 g/L solids prior to conducting density analyses. The culture tube was centrifuged for 5 minutes at 1000 rpm. The fraction of biomass at the top of the solution is visually estimated. The two density solutions bracketing 50% were used to interpolate the density of the biomass as follows:

$$\left[\frac{(0.5 - lower\%)}{(higher\% - lower\%)* (high\rho - low\rho)} \right] + low\rho = biomass\rho$$

Because density solution increments were narrow (0.003 g/mL), any errors in visual estimation of biomass quantities had small effects on the calculated average density. Replicate measurements demonstrated standard deviations less than 1% of average buoyant density (the difference between biomass density and liquid density) values. A

photograph of the density test is included as Figure 4.1. A detailed description of the density analytical method and dilution table are included in Appendix A.

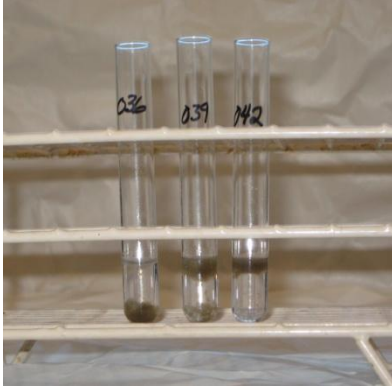


Figure 4.1: Typical activated sludge density test results, with solution densities of 1.036, 1.039, and 1.042 g/mL, and the median biomass density value between 1.036 and 1.039 g/mL.

4.2.4 Carbohydrate Analysis

Total carbohydrate was analyzed using the Phenol method developed by Dubois et al. (1956). This method involves using Phenol to color and concentrated sulfuric acid to digest the sample, which is then analyzed by spectrophotometer at wavelength 490 nm. Dextrose was used as the standard for carbohydrate analysis. A minimum three point standard curve was analyzed with each sample. A detailed description of the carbohydrate analytical procedure is included in Appendix A.

4.2.5 Analytical Practices and Equipment

Three replicates were analyzed per sample for each of the aforementioned analyses. The replicates were used to confirm consistency of the results. The replicates were averaged and used in comparing results between sampling events and between sampling sites.

With the exception of total and soluble phosphorus analyses, all samples were analyzed immediately following each sampling event. Phosphorus and carbohydrate samples were analyzed using an ultraviolet spectrophotometer (Varian, Cary 50, Walnut Creek, CA).

4.3 Filamentous Bacteria Quantification

4.3.1 Image Acquisition

Images of the sludge samples were taken within 24 hours of sample collection, with storage at 4°C. Filamentous bacteria were investigated using two different slide types. First, approximately 20 images were taken of live, unstained activated sludge on a precleaned 25 x 75 mm wet mount slide.

Second, approximately 36 images were taken of live, unstained samples using a hemacytometer slide (Hausser Scientific, Model 3120A, Horsham, PA). The hemacytometer has the advantage of a known volume (0.9 μL) within the 3 x 3 mm grid etched into the slide. These images were used to quantify filament length per mass (FL/TSS in units m/mg) thus relating the filament content to the solids content of each sample.

Images of samples collected between February and April 2008 were taken using a Zeiss Axioskop 40 phase contrast microscope equipped with an AxioCam MRc (Zeiss) color digital camera. The images were acquired through Axio Vision 4.4 at 1388 x 1040 pixels in 24-bit color (RGB) format. Samples collected from May 2008 through the conclusion of the project were taken using an Olympus BX51 phase contrast microscope coupled with an Olympus DP71 color digital camera. These images were acquired using Microsuite Five (Olympus) at 1360 x 1024 pixels in 24 bit RGB format. All images were taken at 100 x magnification.

4.3.2 Image Analysis

Image analysis was performed by three methods. The first method involved visually inspecting the wet mount slide images and ranking the filament abundance using the Filament Index (FI) method developed by Jenkins et al. (2004). The FI was classified on a scale from 0 (no filaments) to 6 (excessive filaments). The FI values for each sample were classified by three individuals and the classifications were averaged.

The second method used an automated image analysis program developed for this study and written using MATLAB image processing software (Image Processing Toolbox 3.1; The Mathworks, Inc., Natick, MA). Preprocessing involved converting the color images to binary form and performing a thresholding operation, separating aggregated biomass (floc) from protruding filamentous structures, and debris elimination. Processing

involved calculating the area of the aggregated biomass and the length of protruding filaments (FL/FA in units 1/μm).

The third method involved manually tracing hemacytometer filament images using a digitizing pad (Intuos 3, Wacom, Ltd, Saitama, Japan) and Adobe Photoshop (V7.0) and subsequently analyzing these traced images using Image J 1.38x (National Institutes of Health, Bethesda, MD). Due to the presence of the grid pattern on the hemacytometer slide, the automated MATLAB program was not successful at quantifying these images, and so they were analyzed by manual tracing of filament lengths and floc areas only. Once a total filament length was obtained from the traced images, the FL/TSS was calculated as follows:

$$\frac{\text{TotalFilamentLength}(\mu\text{m})}{\text{SampleDilution} * 0.9\mu\text{L}} * \frac{10^6 \mu\text{L}}{L} * \frac{L}{\text{TSS}(\text{mg})} * \frac{m}{10^6 \mu\text{m}} = \frac{\text{FL}(m)}{\text{TSS}(\text{mg})}$$

4.3.3 *Filament Index and Filament Length per Floc Area Correlation*

The relationship between FL/FA and the Jenkins FI scale was determined by manually tracing the filament length and floc area for each image of the six (FI = 1 through 6) images published in Jenkins et al. (2004), using a Intuos 3 digitizing pad (Wacom, Ltd., Saitama, Japan) and analyzing the traced images using Image J 1.38x (NIH, Bethesda, MD). The tracing procedure was conducted by three separate investigators and the results of all tracings were averaged.

The Jenkins FI values were also related to FL/FA values based a survey of untrained laymen (undergraduate and graduate students in a wastewater treatment course). 28 microscope images from the full scale investigation covering a broad range of filament content were selected, and 16 people ranked the images using the Jenkins FI key, and these rankings were averaged. The images were also quantified using both the automated MATLAB program and the manual tracing method previously discussed.

4.4 *Statistical Analysis*

Two-sample unequal variance t-tests were performed to evaluate differences between groups of data, including seasonal variations in DSVI, density, and filaments. Linear regressions, non-linear correlations, and t-test analyses were performed using Microsoft Excel (2007). Multivariate correlations were performed using gnuplot (Williams and Kelley, 2007). Correlations were considered statistically significant at a 95% confidence interval ($p < 0.05$).

CHAPTER 5

SEASONAL EFFECTS ON BIOMASS DENSITY AND SETTLEABILITY

5.1 Introduction

Secondary clarification (the removal of microbial biomass produced in upstream bioreactors through sedimentation) can be the most limiting and therefore problematic component of activated sludge wastewater treatment. It is widely accepted that excess filamentous bacteria are the common cause of bulking (poor compaction) in these systems and most research on controlling settling problems has focused on controlling filamentous growth (Martins et al., 2004a). The effects of physical parameters such as floc size and composition, on settleability have also been extensively researched (Andreadakis, 1993, Liao et al., 2001, Liao et al., 2006, Jin et al., 2003, Wilen et al., 2008). While this body of research has greatly advanced our understanding of biosolids sedimentation bulking sludge remains a recurring problem.

Seasonal variations in biomass settleability across a range of suspended culture wastewater treatment technologies, including conventional (aerobic) activated sludge, activated sludge systems with selectors, nitrification/denitrification systems, EBPR, and MBR have been observed (Andreasen et al., 1996; Kruit et al., 2002; Gravaleau et al., 2005, Al-Halbouni et al., 2007). In general, poorer settling performance (as indicated by higher SVI values) has been reported during winter months, while improved settling has been reported during the summer. On the other hand, Wilen et al. (2008) found no

seasonal variations in settleability in full-scale activated sludge wastewater plant performing nitrogen removal with predenitrification and post-nitrification in a trickling filter, as well as phosphorus removal through precipitation in the primary clarifier. These results demonstrate that seasonal variations in settleability are common but not universal in full-scale plants.

In agreement with fundamental settling principles, recent research has demonstrated that variable biomass density (mass per biomass volume) can also significantly impact activated sludge settling (Schuler and Jang, 2007a,b). Andreasen et al. (1996) observed that plants performing EBPR routinely experienced improved settling in the absence of changes in filament content and hypothesized that increased biomass density from increased polyphosphate storage was the cause, although density was not measured. This was recently confirmed in surveys of full scale wastewater treatment systems demonstrating that biomass density varies with plant process configuration and operation to a degree sufficient to significantly affect settling rates (Jang and Schuler 2007, Schuler and Jang, 2007a). Among other findings, this work suggested that improvements to settling observed with installation of anaerobic selectors may at least be partially due to increased density from increased polyphosphate content via EBPR, as was also demonstrated in laboratory EBPR systems (Schuler et al., 2001). SRT and NVSS content were also found to be correlated with density.

It was hypothesized that seasonal variations in density may occur in full scale treatment systems and that these variations may help to explain observed seasonal variations in

settleability. The objectives of this research were to (1) determine the seasonal variations in settleability, density, and filament content at full-scale WWTPs, (2) determine factors contributing to any observed variations in density, including biomass characteristics and plant configuration, and (3) determine how density and filament content may combine to contribute to variable settleability in full scale systems. Seven full scale wastewater treatment systems with a variety of configurations were monitored to achieve these objectives.

5.2 *Materials and methods*

Seven wastewater treatment plants were included in the seasonal variation study (six were monitored for over one year, and one was monitored for seven months). These systems included two conventional activated sludge plants (CAS1 and CAS2), two activated sludge plants equipped with anoxic selectors (AX1 and AX2), the activated sludge plant with an anaerobic selector designed for nitrification/denitrification and EBPR (AN), and the two MBR plants (MBR1 and MBR2). A summary of the configuration of systems, flow capacity, average flow rate, and range of SRT values is included in Chapter 4, Table 4.1.

Plant AN was brought on-line in August 2008, so a complete set of seasonal data was not obtained; however, it was included in modeling and regression analyses relating density, filament content, and settleability. Although the MBR plants do not include secondary

sedimentation, they were included to evaluate how differences in reactor operation affect fundamental biomass characteristics.

Samples were collected at least once per month from February 2008 through February 2009 from near the outlet of the most downstream bioreactor for all plant except AN, for which sampling was August 2008 through February 2009. Samples were analyzed for TSS, VSS, total and soluble phosphorus, total carbohydrate, biomass density, and DSVI. NVSS is the difference between TSS and VSS and non-soluble phosphorus (Pns) is the difference between total and soluble phosphorus. Filament content expressed as FL/TSS was measured using manual tracing of hemacytometer slide images. Statistical analyses including linear univariate and non-linear multivariate regression was performed to evaluate how density and filaments affect settleability and how NVSS, Pns, and temperature affect density. A detailed discussion of the analytical and statistical methods is provided in Chapter 4.

5.3 *Results and discussion*

5.3.1 *Seasonal Variations*

In the four activated sludge plants monitored for one year, biomass density values were significantly higher in warm weather months. Biomass density measurements over the course of one year varied between wastewater facilities and across time. Warm weather values were significantly larger than cold weather values in all four activated sludge (AS) plants, including both conventional and anoxic selector plants, but not in either of the

MBR plants (Figure 5.1). The “warm” months shown in Figure 5.1 are the months with the warmest mixed liquor temperatures (June through October, when average mixed liquor temperatures in plant AX1 were greater than 23.5 degrees) and the “cold” months had the coldest mixed liquor temperatures (December through April, when mixed liquor temperatures in plant AX1 were less than 21 degrees). Mixed liquor temperatures lagged ambient air temperatures somewhat, since the subsurface provides buffering against changes in air temperatures: the coldest ambient average monthly temperatures occurred November through March, and the warmest were May through September (Figure 5.2).

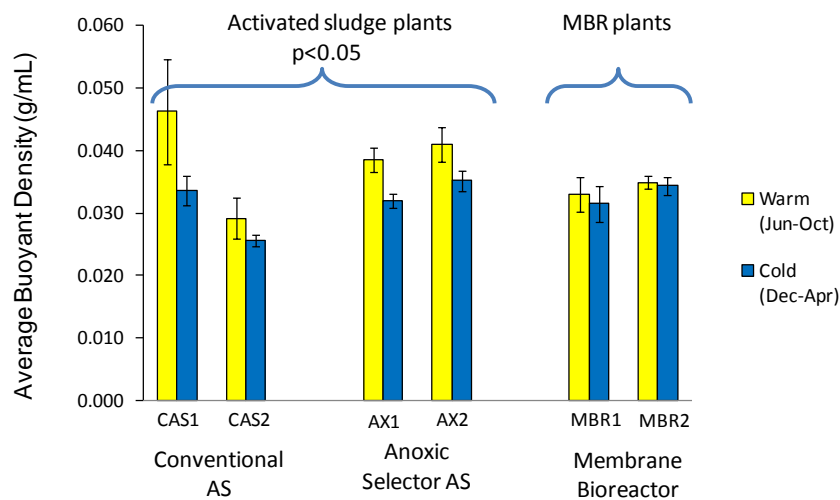


Figure 5.1: Warm and cold weather average biomass density values for four full-scale AS plants and two MBRs.

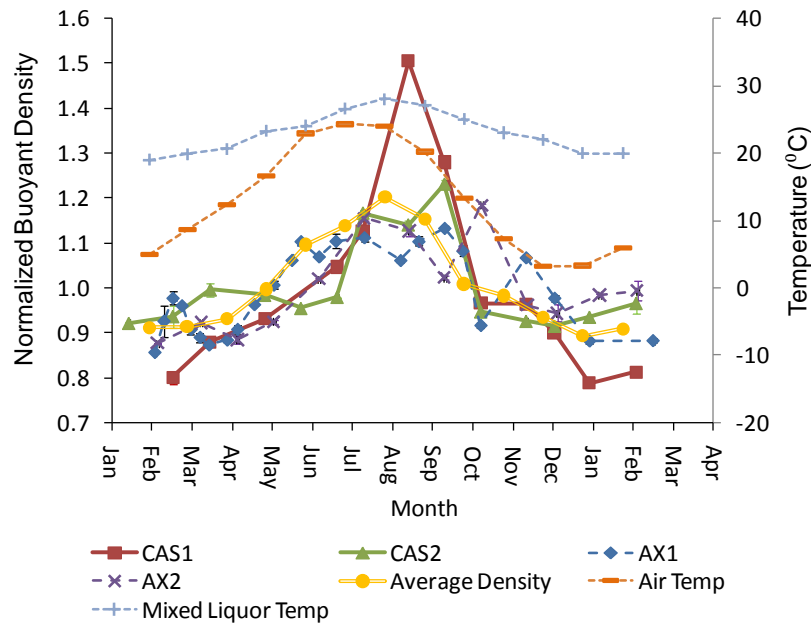


Figure 5.2: Seasonal variation of buoyant density in four AS systems. Buoyant density values are normalized to the yearly average value of each plant. “Average density” is the average of all four plants.

Density measurements exhibited a cyclic seasonal trend in the four activated sludge plants, following the ambient and mixed liquor temperatures (Figure 5.2). These trends did not occur in the MBR plants (data not shown). Buoyant density (biomass density minus liquid density) values shown in Figure 5.2 are normalized to the yearly average of each plant to facilitate comparison of the data. Peak values in all of these plants occurred in the warmest months (July or August) and minimum values occurred in the coldest months (January or February).

Biomass density was positively correlated with wastewater temperature in plant AX1, the plant for which wastewater temperatures were readily available (Figure 5.3). Water density decreases with temperature at values greater than 4 degrees C, which will tend to

increase temperatures effects on buoyant density. Figure 5.3 shows that the slope of the linear regression best fit line increases by about 25% (from 0.00095 g/(mL deg C) to 0.00119 g/(mL deg C)) when the temperature-corrected water density is used to calculate the buoyant density, reflecting field conditions (in all other figures showing buoyant density, the water density is assumed to be 1 g/mL, since all measurements, including those for density and settleability, were performed at constant temperature in the laboratory). Assuming settling velocity is linearly correlated with buoyant density (as in most settling models), the temperature effect on biomass density in plant AX1 was therefore about 4x the temperature effect on water density, but both of these trends are expected to work together to decrease settling velocity with decreasing temperature in the activated sludge plants.

Furthermore, water viscosity increases with increasing temperature, and settling velocity models (such as the Stokes relationship for settling of a discrete sphere) generally suggest settling velocity is inversely related to viscosity, which tends to exacerbate the negative effects of decreasing temperature on settling velocity due to effects on buoyant density. To give an idea of the relative magnitude of viscosity effects, it was calculated that for the data shown in Figure 5.3, the settling velocity of a sphere (assuming Stokes-type settling) would increase approximately 53% as temperature increased from 19 to 28 degrees C, with 42% of this effect due to changes in biomass density, 11% due to changes in water density, and 47% due to changes in water viscosity.

Average ambient air temperatures for the two weeks preceding each sample event for activated sludge plants CAS1, CAS2, AX1, and AX2 (Figure 5.4) in agreement with the results shown in Figures 5.2 and 5.3. The relative magnitude of biomass density, water density, and viscosity described above will vary with range of temperature change and with the plant-specific effects of temperature on biomass density illustrated in Figure 5.4.

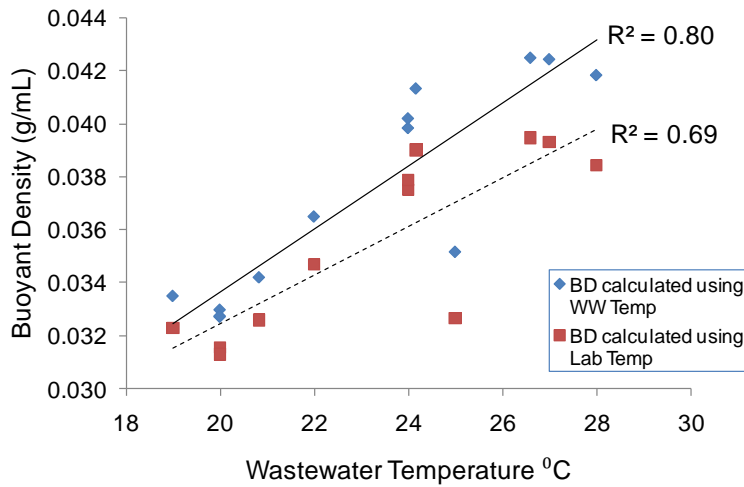


Figure 5.3: The relationship between wastewater temperature and buoyant density in Plant AX1.

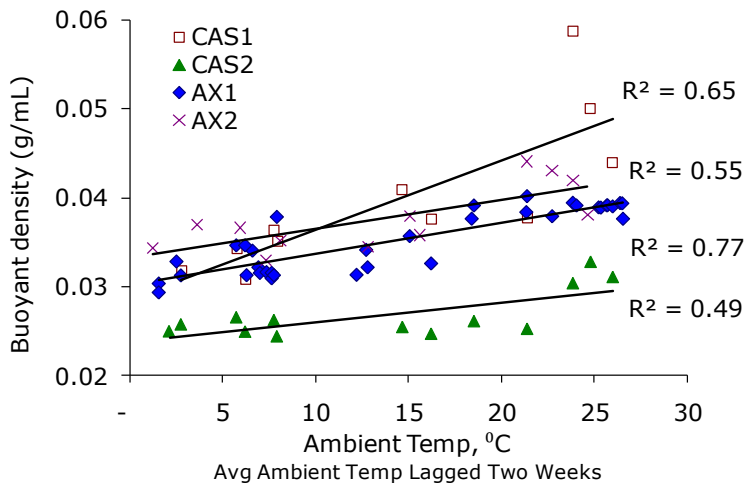


Figure 5.4: The relationship between buoyant density and average ambient temperature (lagged two weeks) for the four activated sludge plants.

The cause of the observed lack of seasonal variability in density in the MBR plants is not known. While the MBR plants had high SRTs (>25 days), the treatment reactor solids were characterized by relatively low NVSS/VSS (average 0.23 mg/mg) and buoyant density (average 0.033 g/mL). This was in contrast to the two AS systems (CAS1 and AN) which also had high SRTs (>18 days) but consistently demonstrated higher NVSS/VSS (average 0.38 mg/mg) and buoyant density (average 0.044 g/mL). Therefore, it appears that high SRT does not result in a similar influence on the biomass in MBR as compared with AS systems. A possible hypothesis for the seasonal variation in activated sludge but not in MBR systems relates to possible bacterial selection mechanisms imposed by the different solids separation techniques. It is reasonable that secondary clarification (gravity separation) retains bacteria with higher NVSS (and higher density) while lower NVSS (lower density) bacteria leaves with the secondary effluent and that seasonal changes in density, NVSS, and temperature perpetuate this selection. In contrast, membrane filtration does not rely on gravity separation and would not promote similar bacterial selection. It is also noteworthy that neither the MBR nor the CAS systems had primary sedimentation, and so high density, non-volatile particulates would have tended to be concentrated by the high SRTs used in all four of these systems. The differences in observed behavior between these systems could therefore have been related to differences in the collection system and raw wastewater characteristics of these systems.

Seasonal variation in settleability was detected in some, but not all activated sludge plants, consistent with previous research summarized above. DSVI values were

significantly lower in warm weather than in cold weather ($p < 0.01$) for plants CAS1 and AX1, but this was not true for plants CAS2 and AX2 (Figure 5.5) although $p = 0.06$ for plant AX2 data. Plant CAS2 experienced a grease related upset during the summer of 2008 that negatively affected settling performance (increasing SVI values), without substantial changes in filament content. The MBR plants did not demonstrate significant seasonal variability in settling performance, but settleability was highly variable in these systems, as indicated by their associated large error bars in Figure 5.5.

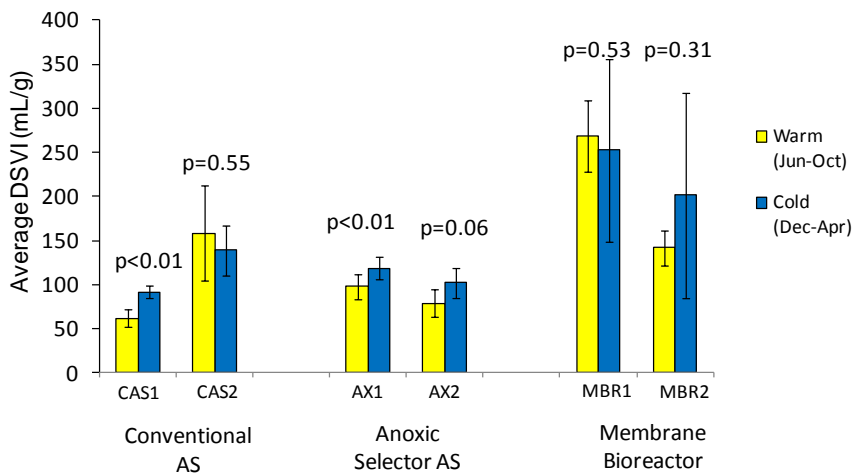


Figure 5.5: Comparison of warm and cold weather average settling data.

Significant seasonal variation in filamentous bacteria content was only observed in plant AX1 ($p < 0.05$), where cold weather filament length per mass values were greater than warm weather values. Significant seasonal variation in filament content was not observed in any of the MBR or other activated sludge plants, although plant AX2 exhibited a nearly significant seasonal filament variation at $p = 0.07$. Filament contents in the activated sludge plants ranged from few to very common (FI 0.5 to 3.5), according to the FI scale (Jenkins et al., 2004), and they ranged from 6.5 to 94 m/mg as determined

from the hemacytometer data. Filament index values of abundant or excessive filaments (FI > 4) were not observed in the AS plants.

5.3.2 Density and Filament Effects on Settleability

The combined influence of biomass density and filament content on settleability was evaluated using an empirical model (Eqn. 1) which was determined to fit measured data well in a separate lab-scale study (Schuler et al., in preparation). The full scale data evaluated with this model were buoyant density (g/mL), FL/TSS (m/mg) and DSVI (mL/g) for five activated sludge plants (CAS1, CAS2, AX1, AX2, and AN) as well as the two MBR plants (MBR1 and MBR2). Nonlinear least-squares regression analysis yielded the constant values of $a = 62.1$ m/mg, $b = 0.58$, and $c = 8.8$ mL/g, with an R^2 value of 0.82 ($p < 0.001$). The plot of this model and measured data is shown in Figure 5.6.

$$DSVI = \left(\frac{a + FL / TSS}{BD} \right)^b + c \quad (1)$$

where a, b, and c are constants

BD = buoyant density

FL/TSS = filament content expressed as filament length/TSS (m/mg)

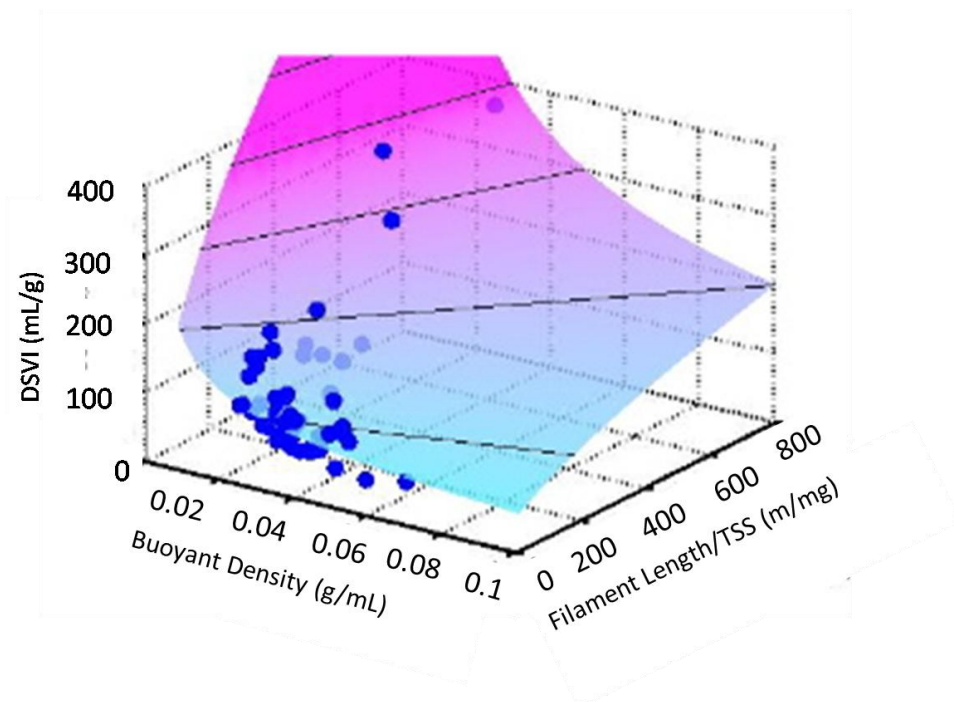


Figure 5.6: Non-linear regression results for empirical model (Eqn. 1) using data from all plants.

Additional modeling was performed using Eqn. 1 to evaluate the correlation of filament content and buoyant density alone as applied to the full data set (AS and MBR plants). The correlation of filament content and settleability (DSVI) was evaluated by setting buoyant density equal to one and resulted in a correlation of $R^2=0.67$ ($p<0.001$). The relationship between buoyant density and DSVI was evaluated by setting FL/TSS equal to zero and resulted in a weak correlation ($R^2=0.17$, $p<0.001$). The MBR plants exhibited high filament content ($FI>4$, $FL/TSS>100$ m/mg) and moderate buoyant density ($MBR1>0.03$ g/mL, $MBR2>0.033$ g/mL). None of the activated sludge plants had sludges characterized by low density (~ 0.02 g/mL) and high filament content, conditions that were found to significantly contribute to poor settleability (high DSVI) by Schuler and Jang (2007a). The inclusion of the MBR data appears to be the major source of the

strong correlation for filament content versus the weak density correlation when related individually to DSVI.

Since seasonal variation in biomass density was only observed in the activated sludge plants, additional modeling was performed excluding the MBR data. The correlation for activated sludge plants using Eqn.1 was $R^2=0.48$ ($p<0.001$) illustrated in Figure 5.7.

Filament length per mass and buoyant density individually correlated with DSVI resulted in $R^2=0.35$ and $R^2=0.38$ ($p<0.001$), respectively.

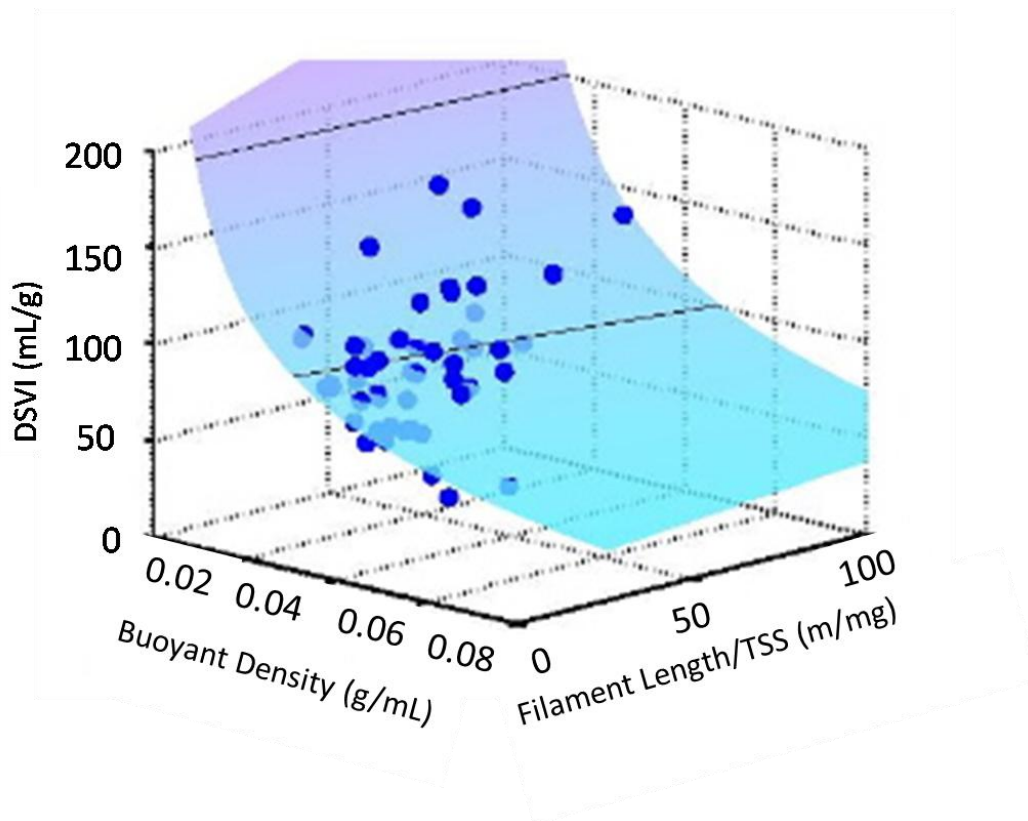


Figure 5.7: Non-linear regression results for empirical model (Eqn. 1) using AS data only (MBR data omitted).

Excluding the MBR data from this analysis indicates that at low to moderate filament content, both buoyant density and filament content influence settleability. The empirical model demonstrates in both cases (evaluation using the full data set and activated sludge plants only) that including both filament content and buoyant density in predicting settleability improves the correlation.

5.3.3 Parameters Affecting Density

The influences of NVSS, biomass phosphorus (Pns) including stored polyphosphate, and total carbohydrate on biomass density were evaluated for each plant. Total carbohydrate was not correlated with biomass density for any of the plants included in this study. Furthermore, the MBR systems did not demonstrate correlations between biomass density and NVSS, or Pns content.

There was a strong correlation ($R^2=0.90$, $p<0.01$) between NVSS/VSS and biomass density for conventional activated sludge plants (Figure 5.8a), consistent with previous results (Schuler and Jang, 2007a). The reason for the high variations in NVSS/VSS in these plants is not certain. Stored polyphosphate can be a major component of NVSS in systems performing EBPR, but this was not the case for the aerobic plants shown in Figure 5.8a, as confirmed by the lack of correlation between Pns and NVSS for these systems (Figure 5.8b). The higher NVSS contents in Plant CAS1 samples, relative to Plant CAS2, may have been linked to the higher SRT in this system (18 to 30 days, as compared to 6 to 8 days in Plant CAS2), which is consistent with previously results from

aerobic systems (Schuler and Jang, 2007a) and with inert biomass accumulation through endogenous decay in extended aerobic systems (Middlebrooks and Garland, 1968).

Further, it is possible that seasonal temperature changes contribute to seasonal changes in non-volatile solids and biomass density through increased endogenous decay during the warm weather conditions when biomass is more active.

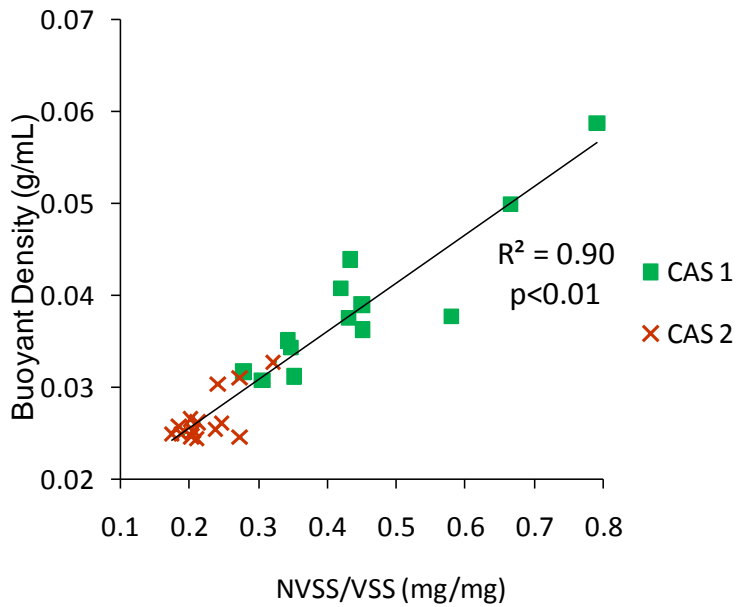


Figure 5.8a: The relationship between buoyant density and NVSS/VSS for conventional AS plants.

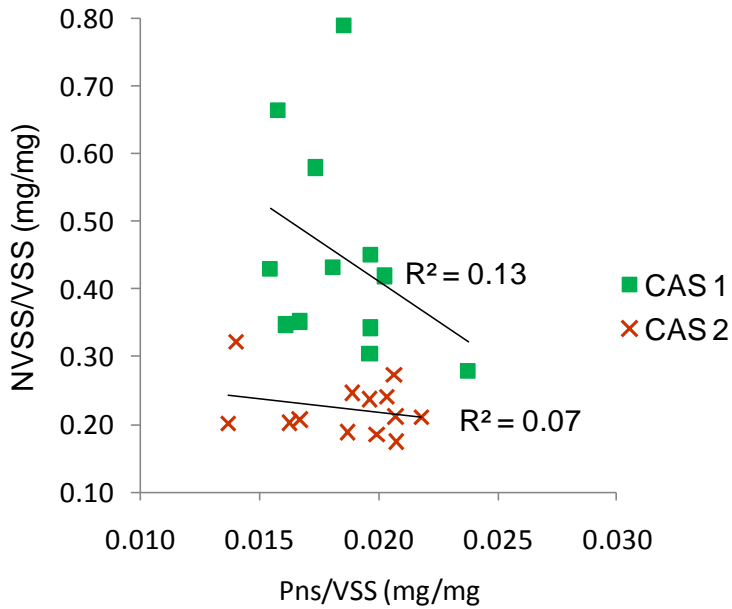


Figure 5.8b: The relationship between NVSS/VSS and Pns/VSS for conventional AS plants.

NVSS/VSS was also correlated with density in the three selector plants ($p \leq 0.01$ in for each plant, Figure 5.9a), including the anaerobic selector AN, which was not included in the seasonal analyses because this plant started up operations mid-way through this study. The three selector plant data sets were offset from each other; the reasons for this are not certain, but this suggests that components of the biomass other than NVSS were contributing to density. The offset towards higher density values in plant AN may have been linked to this plant's operation as an EBPR system, which is expected to increase the content of polyphosphate, glycogen and polyhydroxyalkanoates (PHAs) in the biomass (Mino et al., 1987), all three of which are known to be of higher density than typical bacterial biomass (Mas et al., 1985). Since the latter two components are part of the VSS, their accumulation in the biomass may have contributed to the higher biomass

densities of plant AN samples relative to plants AX1 and AX2 with respect to their NVSS/VSS values, as shown in Figure 5.9a.

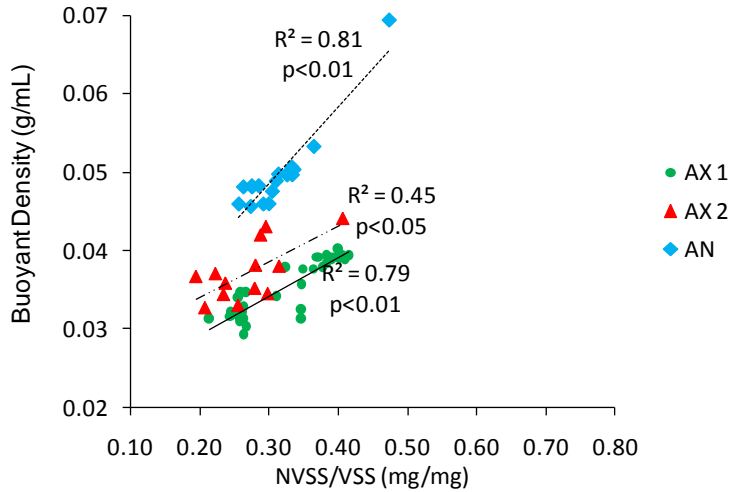


Figure 5.9a: The relationship between buoyant density and NVSS/VSS for selector AS plants.

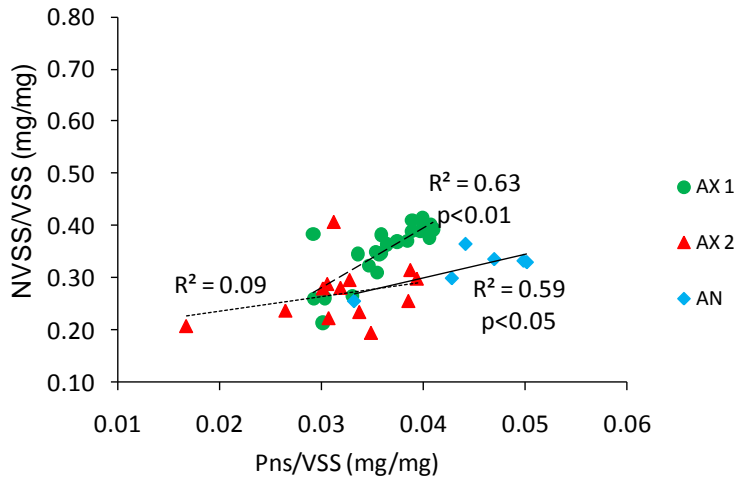


Figure 5.9b: The relationship between NVSS/VSS and polyphosphate content (Pns/VSS) for AS plants with anoxic (AX1 and AX2) and anaerobic (AN) selectors.

Because polyphosphate accumulation is a component of the NVSS that is known to increase biomass density (Suresh et al., 1985, Schuler et al., 2001, Schuler and Jang, 2007a), the contribution of Pns to NVSS was evaluated. Pns content was positively correlated with NVSS for anoxic selector plant AX1 and anaerobic selector plant AN, but

not for plant AX2 (Figure 5.9b). Plant AX2 operates at greater than its design capacity, which could have contributed to greater process variability. Non-EBPR plants are expected to contain approximately 2 to 3% Pns/VSS (Schuler and Jang, 2007a); the typically higher values shown in Figure 5.9b suggests that all three selector plants had at least intermittent EBPR activity, although only plant AN was designed and operated for this process.

5.4 Conclusions

The principal conclusions obtained from this study of the seasonal variation of sludge characteristics include:

- 1) Biomass density was significantly higher in warm weather than in cold weather ($p < 0.05$), it exhibited a consistent seasonal cycle that followed ambient and wastewater temperatures, and it was positively correlated with non-volatile solids in all four full scale activated sludge plants included in this study. None of these trends were evident in two full scale MBR systems.

- 2) Both density and filament content affected settleability. An empirical model of settleability (DSVI) as a function of buoyant density and filament content fit measured data with an R^2 value 0.82. This correlation is notably stronger than modeling settleability as a function of filament content or buoyant density individually. This

demonstrates that accounting for both filament content and buoyant density can greatly improve the ability to predict DSVI.

3) Biomass density was correlated with NVSS content in all activated sludge plants, consistent with previous work. All of the selector plants exhibited some degree of EBPR, as indicated by elevated phosphorus in the biomass (Pns), and Pns content was correlated with NVSS in the anaerobic selector plant and one of the anoxic selector plants. These results suggest that seasonal variability in density may be a consistent phenomenon in full scale activated sludge systems, whether or not such systems include selectors. Monitoring of density, along with filament analyses, may help to diagnose the causes of seasonal variations in settleability when they become problematic and may aid in the development of remedial strategies (such as methods to increase NVSS content).

CHAPTER 6

DAILY CHANGES IN BIOMASS DENSITY AND SETTLEABILITY AT FULL-SCALE SELECTOR WASTEWATER TREATMENT FACILITIES

6.1 *Introduction*

Seasonal variation in settleability has been demonstrated in numerous studies (Andreasen, et al., 1996; Kruit et al., 2002; Al-Halbouni et al., 2007). It has also been demonstrated that settleability can vary on a weekly and even daily time scale. For example, studies of full scale activated sludge plants, including systems equipped with anoxic and anaerobic selectors, demonstrated that settling characteristics can vary over the course of days (Gabb et al., 1991, Parker et al., 2004). Vanderhasselt et al. (1997) found that changing lab scale process parameters, such as aeration intensity, could change settleability over the course of hours. While these studies reported observed short-term settleability variations, they did not evaluate whether these changes were recurring, cyclical, or possibly upset related.

Pitman et al. (1983) found that phosphorus removal performance degraded at some plants performing EBPR following weekend low flow conditions. The occurrence of such cyclic EBPR performance is referred to as “Monday Peak” phenomena. Other studies investigated EBPR performance under low loading conditions to ascertain what factors contributed to increased effluent phosphorus. A 1998 laboratory scale study using an anaerobic-aerobic-settling sequencing batch reactor by Brdjanovic et al. found that

excessive aeration under low loading conditions results in (1) a depletion of PHB that inhibits phosphorus uptake when loading conditions return to normal; (2) an increase in the ratio of polyphosphate to PHB in the cells which further inhibits aerobic phosphorus uptake; and (3) a deterioration of EPBR performance when normal loading resumes because phosphorus release in the anaerobic reactor continues. Apparently, the polyphosphate accumulating organisms (PAOs) were unable to recover quickly enough to prevent a lag in phosphorus uptake.

Since wastewater facilities equipped with anoxic or anaerobic selectors have been demonstrated to perform varying degrees of EBPR (Lugowski et al., 2007), it was hypothesized that low loading conditions that occurring during weekends may lead to “Monday Peak” phenomena. It was further hypothesized that, since polyphosphate storage is known to influence biomass density, such temporary degradation of EBPR performance may result in corresponding decreased density and degraded settleability.

The objectives of this research were to determine if biomass density is variable on a weekly basis and whether this variation affects settleability due to the existence of Monday Peak phenomena. Daily sampling was conducted to evaluate possible density and settling changes that occur in conjunction with variable weekly flow conditions at two of the selector equipped plants included in this study.

6.2 *Materials and Methods*

Three weekly sampling events were initiated during this research. The first daily sampling event was conducted at plant AX1, equipped with an anoxic selector, from March 16 to 19, 2008 (Sunday through Wednesday). During this sampling event, a full week of sampling was not completed due to complications with laboratory equipment. The second daily sampling event was also conducted at plant AX1 from June 21 to 27, 2008 (Saturday through Friday). The third daily sampling event was conducted at plant AN equipped with an anaerobic selector from January 11 to January 14, 2009 (Sunday through Wednesday). Daily sampling was suspended during this event due to a plant upset event that began January 15, 2009. The conditions and results of this upset and recovery are discussed in detail in Chapter 7.

Activated sludge samples were collected from the same location and at approximately the same time each day. Samples were analyzed for TSS, VSS, total and soluble phosphorus, total carbohydrate, biomass density, and DSVI. Filament content was evaluated by visual inspection of microscope images using the filament index method (Jenkins et al., 2004).

A detailed description of the analytical protocols is provided in Chapter 4.

6.3 Results and Discussion

This section is organized to address the daily sampling events at wastewater plant AX1 and AN separately. Temporal density, settling, and non-soluble phosphorus content trends and influencing parameters are addressed for each daily sampling event.

6.3.1 Plant AX1 – March and June 2008 Sampling Events

Daily samples were collected from plant AX1, equipped with an anoxic selector, on March 16 through 19, 2008 (Sunday through Wednesday) and June 21 through 27, 2008 (Saturday through Friday). The March 2008 sampling event was terminated after four days due to laboratory equipment problems.

Monday Peak phenomena were not detected in either sampling event, and so the hypothesis that short-term degradation of EBPR because of such peaks may lead to short-term degradation of settleability could not be tested. Buoyant density did not vary substantially during either the March or June daily sampling events (Figure 6.1). Settleability and buoyant density did not correlate during the March or June 2008 sampling events (not shown). Settleability and soluble phosphorus varied during the March sampling event but only soluble phosphorus varied during the June sampling event (Figures 6.1 and 6.2). A 56% decrease in soluble phosphorus content and 13% increase in settleability (measured as DSVI) were detected on Tuesday, March 18 and Wednesday, March 19, respectively. The average filament index ranking for the March sampling

event increased from 2.8 to 3.2 between Tuesday and Wednesday which could have contributed to the increased DSVI on March 19.

A 29% increase in soluble phosphorus was observed on Wednesday, June 25 (Figure 6.2); however, there was no apparent variability in either buoyant density or settleability during the June study (Figure 6.1). On June 25, five wastewater plants were sampled with plant AX1 being the first. As a result, there was an approximate 3 hour difference between sample collection and soluble phosphorus analysis for this plant. A review of plant performance data indicates that wastewater flows were very consistent during the June sampling event. Even though samples were kept on ice during transportation, the increased soluble phosphorus on this date is more likely a result of phosphorus leakage in the activated sludge sample than indicative of a Monday peak type event.

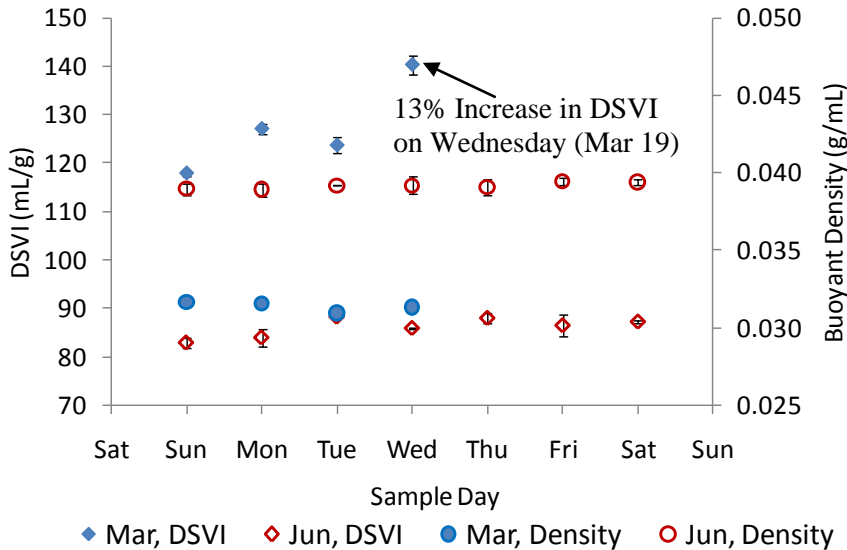


Figure 6.1: Daily variation in DSVI and buoyant density for the March and June 2008 sampling events at plant AX1.

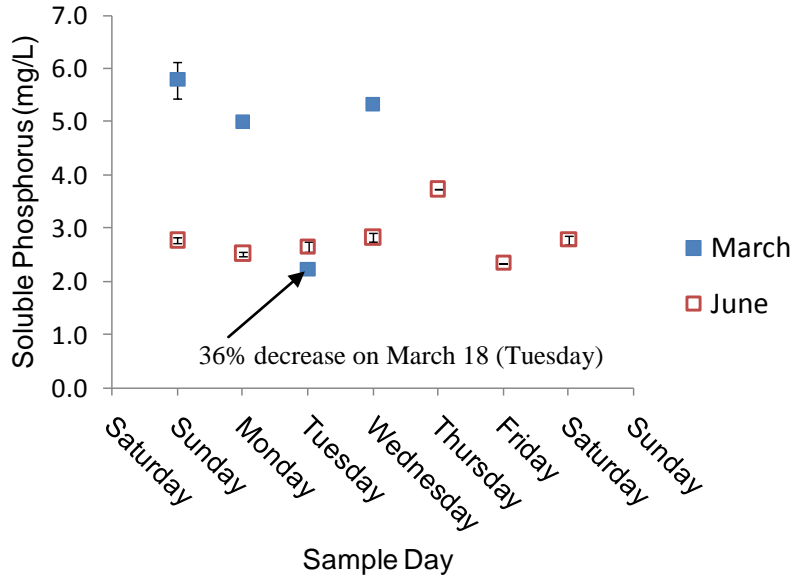


Figure 6.2: Daily variation in soluble phosphorus content for the March and June 2008 sampling events at plant AX1.

6.3.2 Plant AN - January 2009 Sampling Event

Similarly negative results with respect to a lack of evidence for Monday Peak phenomena were found at Plant AN, which included an anaerobic selector. Daily samples were collected from this plant January 11 through 14, 2009 (Sunday through Wednesday).

Temporal trends for buoyant density, settleability, and soluble phosphorus were plotted and are included in Figures 6.3 and 6.4. Buoyant density and settleability did not vary substantially over the four day sampling event. Soluble phosphorus was variable during the January sampling events with the highest concentrations detected on Sunday, January 11 and Wednesday, January 14; however it should be noted that the highest soluble phosphorus detection was 1.2 mg/L which is within the range of soluble phosphorus detected at this plant since operation began in August 2008. Further, there was an

approximate two hour delay in transporting the January 11 and 14 samples to the laboratory which may have resulted in minor phosphorus leakage from the activated sludge sample.

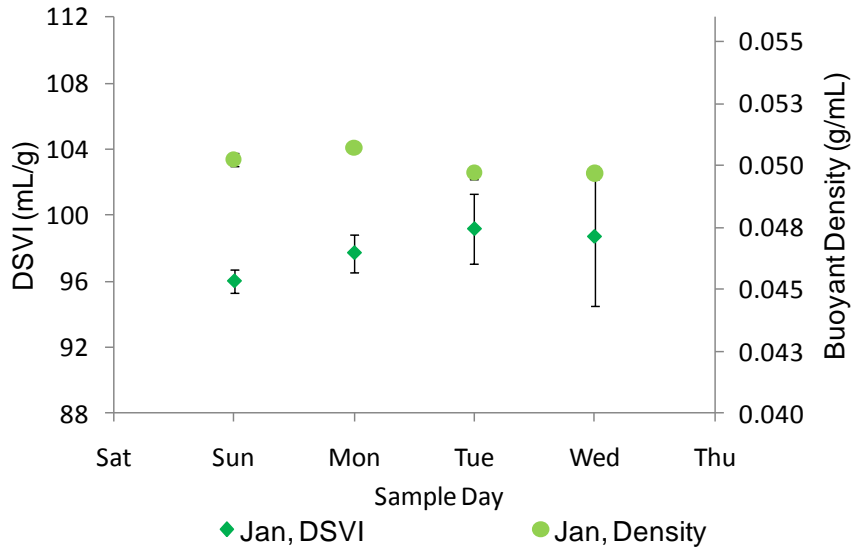


Figure 6.3: Daily variation in settleability and density at plant AN (January 2009).

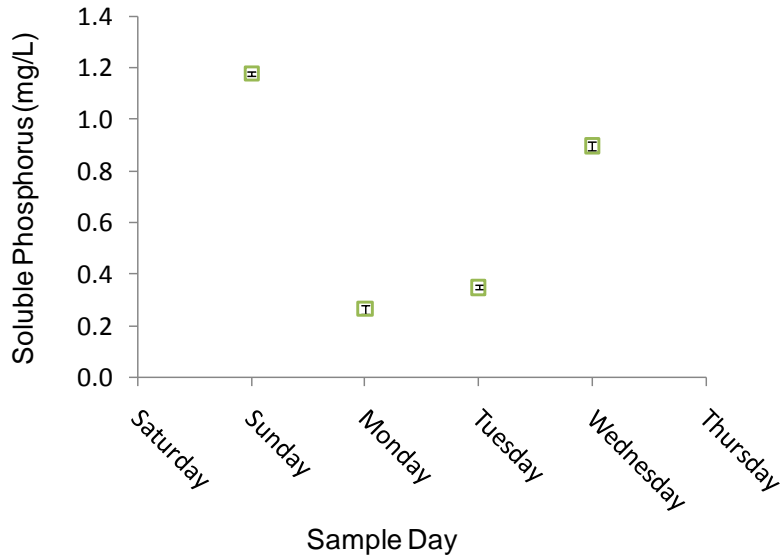


Figure 6.4: Daily variation in soluble phosphorus content at plant AN (January 2009).

A Monday peak phenomena was not observed at Plant AN during the January 2009 sampling event. Plant AN serves a small community and does experience an approximate 20% decrease in wastewater flow over the weekend. However, this flow variation did not appear to negatively affect EBPR or settling during the sampling period.

6.4 Conclusions

This chapter addresses findings of three separate daily sampling events conducted in March 2008, June 2008, and January 2009 at two full-scale wastewater plants, one equipped with an anoxic selector (AX1) and the other equipped with an anaerobic selector (AN). It has been demonstrated that plants equipped with selectors are capable of performing various degrees of EBPR. Also, cyclical changes in phosphorus removal have been demonstrated at EBPR plants with low weekend flow conditions. Since polyphosphate content has been directly correlated with biomass density and density is known to influence settleability, cyclical changes in phosphorus removal performance also have the potential to influence settling. Daily sampling events were conducted to evaluate the possible occurrence of Monday peak phenomena at these plants.

While variable settling and phosphorus content was observed during parts of this study, buoyant density consistently remained stable for each sampling event. Daily sampling events conducted at plants AX1 and AN indicate that Monday peak phenomena do not occur at these facilities, and so the hypothesis that Monday peaks may lead to temporarily degraded settleability was not tested.

CHAPTER 7

PROCESS START-UP AND UPSET EFFECTS ON BIOMASS DENSITY AND SETTLEABILITY

7.1 *Introduction*

Production of well-settling biosolids is therefore critical to providing a high quality effluent, and also to the biological treatment process, since a portion of the settled solids is returned to biological reactors. Wastewater process start-up requires close monitoring and consistent adjustment of operating parameters to get the system to a stable operating condition as quickly as possible (Metcalf and Eddy, 2003). In contrast, process upsets in activated sludge treatment can result in rapid degradation of effluent quality, and they can be caused by a variety of factors.

The source of the process upset can result from external or internal disturbances.

External disturbances include variations in wastewater flow and composition (such as wet weather high flow, low strength influent) and introduction of toxics that may disrupt biologic processes. Internal disturbances can include filamentous bulking, disruptions due to equipment failure, or planned maintenance (Metcalf and Eddy, 2003). The results of a 1999 survey of wastewater facilities demonstrated that 70% of those surveyed had experienced some form of process upset (Love and Bott, 2000). High flow/low strength loading, acute shock loading from toxic organics, oil and grease, or heavy metals, and influent pH extremes were reported as the most common sources of upset corresponding

and ineffective organics removal, ineffective nitrification, deflocculation (increased effluent solids), and nonfilamentous foaming reported as the most common upset results (Love and Bott, 2000).

Upset events resulting from toxic loading have been less studied, with little or no published studies of full scale upset effects on settling. Tokuz et al. (1991) evaluated how hazardous organic compounds influence activated sludge performance in a laboratory scale system. Love and Bott (2002) conducted a laboratory scale study evaluating microbial stress influences on process upsets. Henriques et al. (2004, 2005, 2007a) presented several laboratory studies evaluating the influence that floc size has on sensitivity to chemical toxins and the degree to which various toxins cause deflocculation. Using metabolic footprinting and statistical analysis, they evaluated the effect of three chemical toxins on activated sludge from four treatment plants to determine probable biomarkers that could be used to indicate process upset (2007b). To our knowledge, there have been no published studies specifically addressing recovery from severe process upsets at full-scale plants, possibly because such events occur without warning and are therefore difficult to study.

Sears et al. (2006), demonstrated that biomass density was correlated with settling velocities within a single activated sludge plant. It has been demonstrated that the buoyant density of the suspended biomass produced in activated sludge systems can vary widely with process configuration, including polyphosphate storage variations due to EBPR performance (or lack thereof; Schuler and Jang, 2007a,b).

There has been no previous research on how biomass density might vary during process start-up and how process upsets may negatively affect biosolids settling through changes to biomass density. It was hypothesized that biomass density will vary during process start-up and contribute to changes in settleability. Further, process upsets were hypothesized to affect EBPR by decreasing polyphosphate storage and hence decreasing biomass density.

The objectives of this research were to (1) determine how biomass density, settling, and other parameters vary during a full-scale process start-up and process upset and (2) determine factors contributing to this variability. Understanding how biomass density, settling and polyphosphate content can change during start-up and upsets to EBPR systems may be important to preventing such upsets and to providing appropriate responses. This study focused on a process start-up and an upset coincidental to a detailed study of settling in a full scale wastewater treatment plant performing EBPR.

7.2 Materials and Methods

7.2.1 Site Description, System Start-up and Sample Collection

The full-scale wastewater treatment facility addressed in this chapter is an AS system equipped with an anaerobic selector (AN). Process configuration, design capacity, and operating parameters are discussed in Chapter 4. This new plant commenced operation on August 12, 2008, with seed from the existing non-EBPR plant. Routine sampling was

initiated on August 27, 2008 as part of a larger investigation of temporal changes in density, filament content, and settleability on daily to monthly time scales.

Activated sludge samples were collected from the end of the treatment basin being aerated at the time of sampling. Samples were kept on ice during transportation and placed in a 22°C water bath upon arriving at the laboratory. Because return activated sludge (RAS) is routed through the single anaerobic selector which discharges equally to the parallel treatment trains, the contents of the treatment trains are mixed.

7.2.2 Process Upset Event

Daily sampling was initiated on January 11, 2009 as part of an investigation to evaluate weekend low loading effects on treatment performance and other temporal effects (see Chapter 6). On January 15, 2009, repair of a leaking air supply line commenced, which included taking one of the two activated sludge trains off-line for 36 hours. During the first 12 hours, aeration was discontinued in the entire plant. During the subsequent 24 hours the cyclic anoxic/aerobic operation was resumed in one of the two treatment trains, and then the second treatment train was returned to service and normal plant operation resumed. A second disruption occurred on January 25, 2009 when the aeration control program briefly malfunctioned, the duration of this disruption is unknown. Activated sludge samples were analyzed every 2 to 3 days from January 11 through February 12, 2009, during system upset and recovery.

7.2.3 Analytical Methods

All samples were analyzed for TSS, VSS, total and soluble phosphorus, biomass density, and DSVI. NVSS was calculated as the difference between TSS and VSS and P_{ns} was calculated as the difference between total and soluble phosphorus. Filament content (filament length per floc area) was quantified from wet mount images (100x phase contrast) using the automated image analysis program developed for this study. Statistical analyses included univariate linear correlations and two-sample unequal variance t-tests. A detailed discussion of the analytical protocols is provided in Chapter 4.

7.3 Results and Discussion

7.3.1 System Start-up Performance

Settleability, density, and filament content demonstrate these parameters were variable for the first two months of the new plant's operation (Figure 7.1). From November 2008 until the system upset event on January 15, 2009, density and settleability were relatively stable but filament content demonstrated a gradual increase. During start-up variations in settleability were attributable to changes in both filament content and biomass density based upon the statistically significant correlation between these parameters (Figure 7.2). The pre-existing system was prone to excessive filamentous growth and poor settling performance. Since the new system was seeded with activated sludge from the pre-existing plant, elevated filament content during start-up should have been expected.

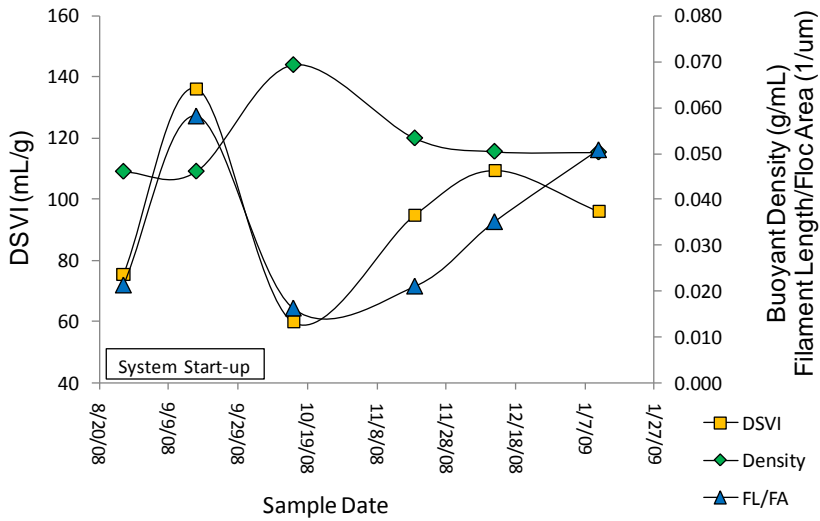


Figure 7.1: Temporal changes in settleability (DSVI), buoyant density, and filament content (FL/FA) for the first six months of system operation.

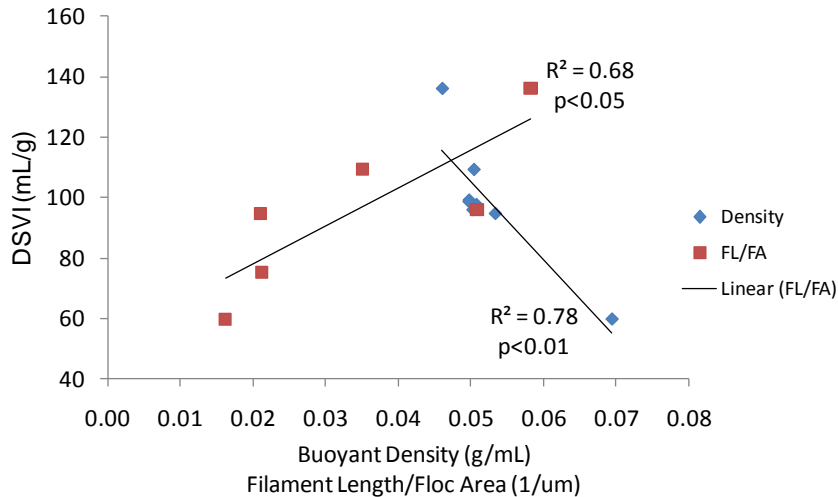


Figure 7.2: The relationship between settleability (DSVI) and buoyant density and settleability and filament content (FL/FA) during plant start-up and stabilization.

Biomass density was strongly correlated with non-volatile solids content (Figure 7.3).

The October 15, 2008 sample followed a rainfall event that appears to have introduced inert solids, based on a substantial increase in NVSS and density without a corresponding

increase in VSS or phosphorus content. This plant is equipped with a grit chamber but no primary sedimentation basin and is sensitive to rainfall events because it services a small community with an aging collection system and many unpaved and/or unimproved (no curb and gutter) roadways. Excluding the October 15 post-rainfall sample, NVSS was positively correlated with Pns content ($R^2=0.61$, $p<0.05$, plot not shown), but density was not as well correlated with Pns ($R^2=0.37$, $p<0.05$, plot not shown). Plant AN was seeded with reactor solids from the previous wastewater treatment plant which was characterized by high NVSS but low Pns indicating that the biomass did not contain an appreciable PAO population. Therefore, it appears that the weaker correlation between biomass density and Pns during start-up and stabilization is related to the growth of PAOs in the new system designed for their selection.

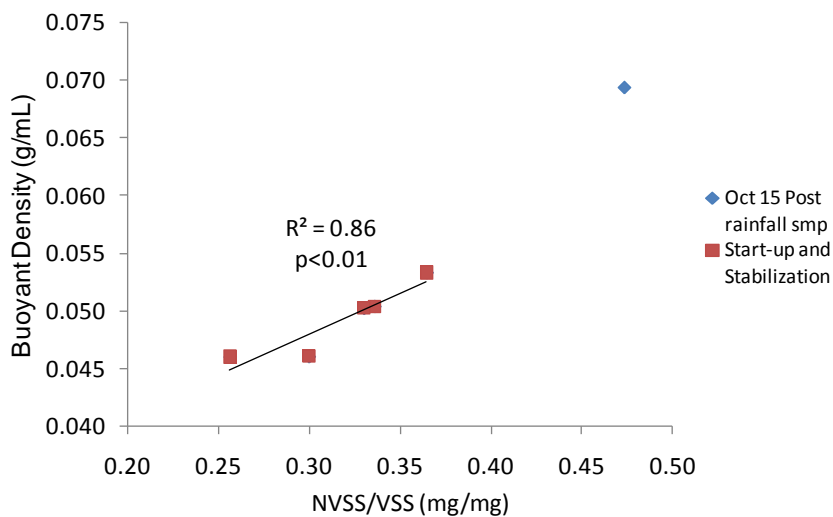


Figure 7.3: The relationship between buoyant density and NVSS/VSS during system start-up and stabilization

7.3.2 *System Upset and Recovery*

On January 15, system repairs required passage of all flow through one of the two treatment trains for 36 hours. Aeration was discontinued in the functional train for 12 hours, followed by normal anoxic/aerobic operation for 24 hours before the second train was brought back online. During this time the functional train was operated at approximately 15 to 30% above its design capacity. When the second treatment train was brought back online it was not seeded with biomass from the operating treatment train and as a result biomass solids were initially very low (TSS < 1,000 mg/L, as compared to the continually operating train at 2,680 mg/L), until equilibration of solids concentrations within approximately two days.

Daily sampling from January 11-14, 2009, just prior to the first upset, demonstrated little change in density, settleability, and filament content (Figure 7.4), and is included to illustrate the degree to which process upset affected system performance. Immediately following the repair related upset, density and filament content decreased and settleability performance degraded (Figure 7.4).

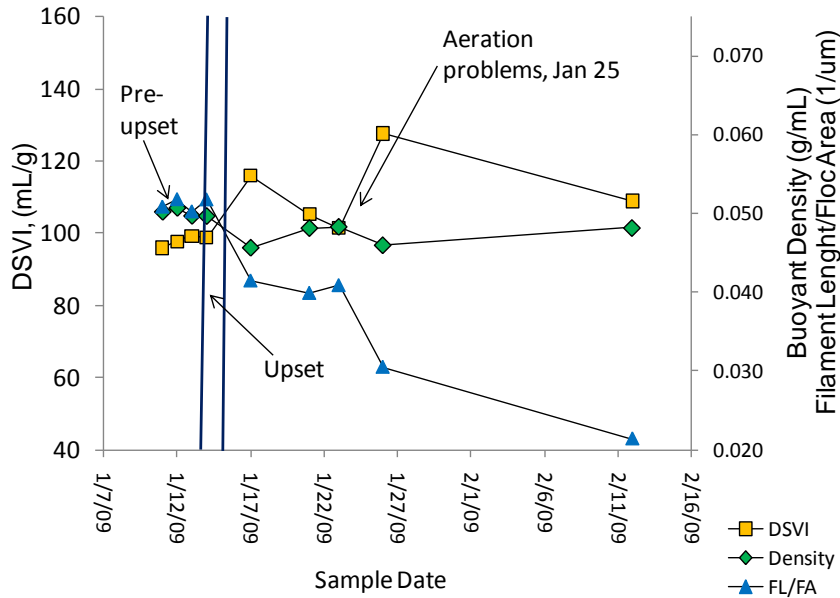


Figure 7.4: Temporal changes in settleability (DSVI), buoyant density, and filament content for the process upset and recovery event.

The 12 hour disruption of the anaerobic/aerobic cycling and the 36 hour decrease in operational reactor volume, negatively impacted EBPR activity. This was evident in the Pns/VSS content, which decreased from 0.0501 ± 0.002 mg/mg before the upset to 0.0284 ± 0.001 mg/mg on January 17, immediately after the system returned to normal operation, which was a 46% decrease in Pns/VSS (Figure 7.5). Simultaneously, density decreased from 0.0501 ± 0.0005 g/mL to 0.0457 ± 0.0001 g/mL (a 10% decrease, Figure 7.5) and NVSS/VSS decreased from 0.33 ± 0.003 mg/mg to 0.273 ± 0.013 mg/mg (an 18% decrease, not shown). All of these changes were significant ($p < 0.05$).

The upset had a negative impact on settleability with DSVI increasing by 21% (Figure 7.4). While settleability degraded as a result of the upset the DSVI remained below 150

mL/g which is considered the upper bound for non-bulking settling. In contrast, effluent TSS increased from 5.8 mg/L pre-upset to 13.7 mg/L on January 19, 2009.

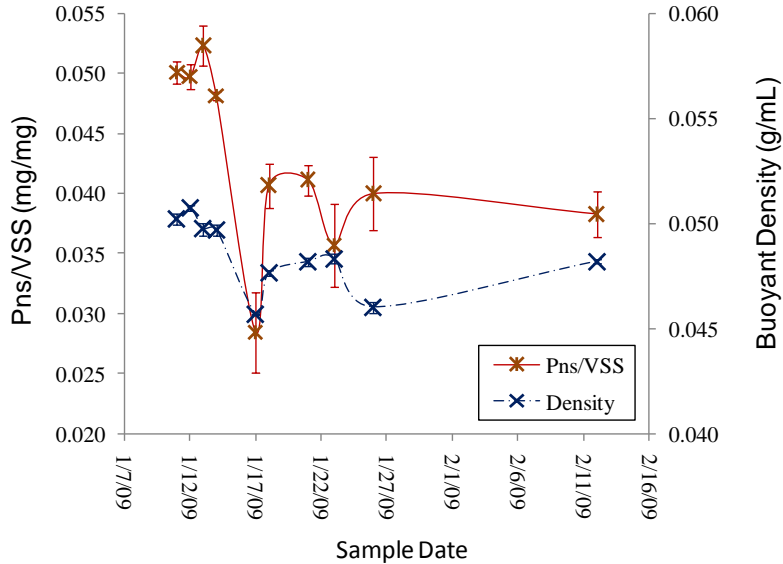


Figure 7.5 Temporal changes in buoyant density and polyphosphate during upset. The immediate change between the pre and post-upset conditions are apparent.

Pns/VSS, NVSS/VSS, and density values recovered to near pre-upset conditions within 48 hours of normal operation resumption (Figure 7.5). The impact the upset had on the activated sludge biomass is evidenced by the sudden and significant decrease in Pns which was simultaneous with biomass density. A second upset due to a brief aeration disruption on January 25, 2009 apparently led to decreased density and increased SVI (Figure 7.4) although a corresponding drop in Pns/VSS did not occur.

Pre-upset (January 11 to 14) data was significantly different from post-upset (January 17 to February 12) data for DSVI ($p < 0.05$) and density, filament content, and polyphosphate (Pns/VSS) values ($p < 0.01$) (Figure 7.6, DSVI not shown). DSVI was inversely correlated with buoyant density both before and after the upset and for the entire data set

(Figure 7.7), consistent with previous research (Schuler et al., 2001, Schuler and Jang, 2007a, b). Substantial research into bulking events has demonstrated that filamentous bacteria can have a negative effect on settling performance (Jenkins et al., 2004, Martins et al., 2004a). In this study, filament content decreased following the upset and there is no post-upset correlation between filament content and DSVI, and therefore did not appear to cause the observed changes in settling.

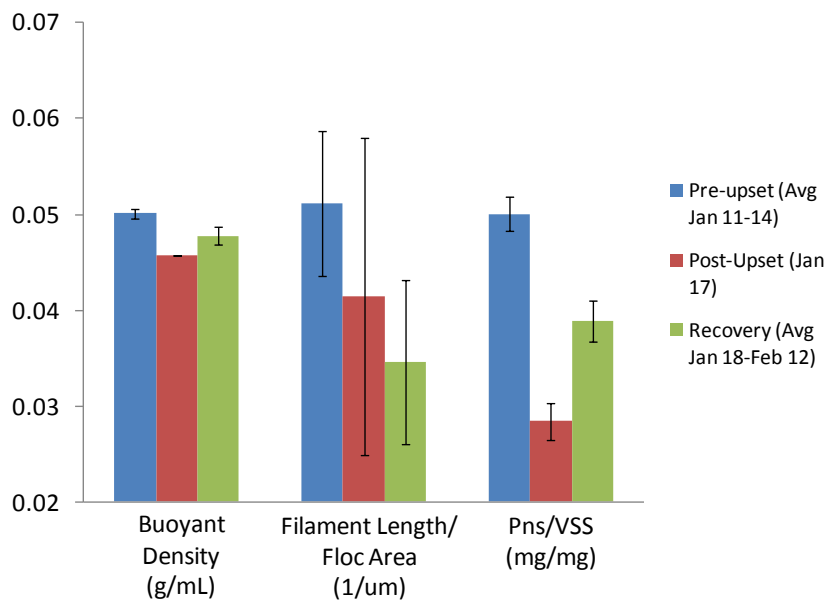


Figure 7.6: Bar chart illustrating density, filament content, and polyphosphate pre-upset averages (Jan. 11-14), post-upset sample (Jan. 17) and post-upset averages (Jan. 18 – Feb. 12).

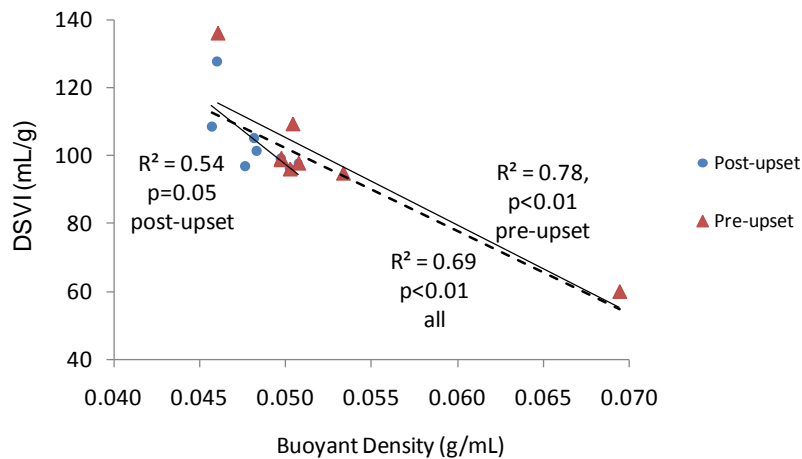


Figure 7.7: The relationship between settleability and density for pre-upset, post-upset, and the entire data set.

The observed changes in density were positively correlated with Pns/VSS and NVSS (p<0.01, Figure 7.8), consistent with previous results (Schuler et al., 2001, Schuler and Jang 2007a). Recovery was also strongly related to increased Pns indicating that polyphosphate accumulating organisms were able to recover within days of the upset.

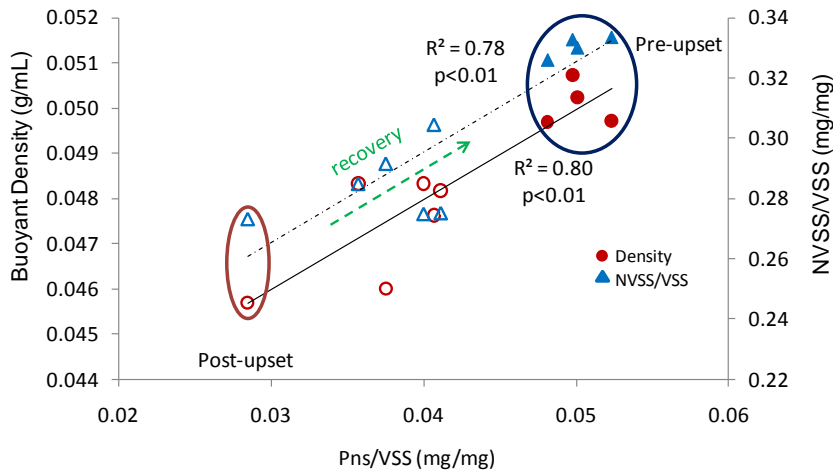


Figure 7.8: The relationship between polyphosphate (Pns/VSS) and both buoyant density and NVSS/VSS. Pre-upset, immediately post-upset (Jan. 17), and recovery conditions are indicated.

7.4 *Conclusions*

This chapter reports the findings of seven months of data collected at a full-scale wastewater treatment plant that captured initial process start-up and stabilization and the occurrence of a winter process upset and recovery. Process start-up demonstrated variable settling conditions influenced both by changes in biomass density and filament content. While the repair related upset was not fortuitous, the timing of a prearranged daily sampling event allowed the researcher to characterize how process upset affected system performance. The upset caused a degradation of treatment performance with respect to settleability, resulting from significant changes in biomass density, and polyphosphate content but little effect due to post-upset filament content.

Process upsets to EBPR systems may result in decreased phosphorus removal, as well as degraded settling characteristics linked to polyphosphate release and consequent decreased biomass density. Polyphosphate and NVSS content have been previously shown to be correlated with biomass density during normal operating conditions of EBPR systems. This study demonstrated that this is true during system upsets, as well, and so monitoring biomass density may be a useful tool in evaluating overall process performance and upset recovery trends, and differentiating between filamentous and density as causative factors in degraded settleability. Biomass density measurement is a simple, repeatable test that could be a useful tool in evaluating conditions under both stable and unstable process operation.

CHAPTER 8
COMPARISON OF IMAGE ANALYSIS METHODS FOR QUANTIFYING
FILAMENTOUS BACTERIA

8.1 *Introduction*

Despite extensive research on secondary settling, it remains one of the most problematic processes in domestic wastewater treatment systems. It is widely accepted that excess growth of filamentous bacteria can hinder settling and is the most common cause of bulking conditions in secondary clarifiers (Jenkins et al., 2004, Martins et al., 2004). A great deal of research into controlling filamentous growth has been accompanied by the development of several methods to quantify filaments.

Filament quantification methods include visual ranking, manual methods such as tracing of images, and automated image analysis. A commonly used visual ranking method developed by Jenkins et al. (2004) involves classifying filament content by FI ranking on a scale from 0 (no filaments) to 6 (excessive filaments). A similar visual ranking method developed by Eikelboom (2000) uses a classification system that ranges from 0 (no filaments) to 5 (very many filaments). FI ranking is commonly used because it is rapid, simple, and does not require specialized equipment other than a suitable microscope. However, due to its subjective nature, the method may be considered less robust than other approaches (Banadda et al., 2005, da Motta et al., 2002).

“Manual” methods to quantify filaments have included counting of the number of intersections between filaments and a vertical line transversing a known volume of sample (Pitt and Jenkins, 1990), tracing filaments on a video screen (Matsui, S. and Yamamoto, R., 1984), and visual estimation of filaments lengths (Palm et al., 1980, Sezgin et al., 1978). Such methods may provide advantages with respect to accurately reflecting filament lengths appearing in microscope images, they can be laborious and time-consuming.

In an effort to reduce the labor involved in filament quantification, procedures for automated image analysis of digital images have been applied by several researchers (Amaral and Ferreira, 2005, da Motta et al., 2002, Jenne et al., 2005, Mesquita et al., 2008, Mesquita et al., 2009). In general, automated filament quantification involves preprocessing operations to separate floc and filaments followed by operations to quantify the extended filament length and floc parameters such as diameter (da Motta et al., 2002), shape measurements including form factor, roundness and radius of gyration (Banadda et al., 2005, Jenne et al., 2005), or total floc area (Amaral et al., 2002, Amaral and Ferreira, 2005, Mesquita et al., 2008). Automated image analysis typically includes a phase contrast microscope equipped with a digital camera and specialized image analysis software and/or development of specialized programs for image preprocessing and processing. The quality of the images can have a significant impact on the analysis where variable background shading, slide and sample debris, etc. can interfere with the automated quantification success. The specialized equipment, current necessity of developing a custom computer program and expertise necessary to perform automated

image analysis has inhibited the broader use of automated approaches by researchers and practitioners.

According to Schuler and Jassby (2007) and Mesquita et al. (2008), quantification methods that relate filament content to biomass solids content (FL/TSS) are the most useful for comparing data from different wastewater sources because length/mass measurement normalizes the filament content to biomass concentration. Further, Amaral and Ferreira (2005) found that the positive linear correlation observed between settleability (SVI) and FL/FA measurements was improved when SVI was correlated with FL/TSS.

The objectives of this research were to determine if the filament index method (Jenkins et al., 2004) could be calibrated to relate subjective visual ranking to a quantitative parameter. Further, this research aims to compare automated image analysis and manual tracing methods to determine relative data quality obtained and to characterize the level of effort involved in each method.

8.2 *Materials and Methods*

Images of activated sludge samples collected from each of the seven wastewater treatment plants included in this study. Images were taken within 24 hours of sample collection, with storage at 4°C. TSS analysis results were used to calculate FL/TSS and settleability (DSVI). A detail discussion of analytical methods was included in Chapter 4.

8.2.1 Filament Index Calibration and Survey Experiment

Jenkins et al. (2004) suggested a 7 point scale for ranking FI content based on microscope imaging (0: none, 1: few, 2: some, 3: common, 4: very common, 5: abundant, 6: excessive), and they included example images for FI values = 1 through 6. Each of these images was manually traced using a digitizing pad (Intuos 3, Wacom, Ltd, Saitama, Japan) and the lengths of traced filaments and areas of bacterial flocs were determined by image analysis software (Image J 1.38x, National Institutes of Health, Bethesda, MD). Non-linear regression analysis was performed to calibrate the FI key to the total filament length/floc area measurements for each image. For calculation of average values and standard deviations manual tracing was performed by three different individuals for each image.

Once a calibration equation was determined for the FI key, a survey experiment was performed to evaluate its application. The FI survey was designed to also evaluate how robust the FI ranking is when employed by a group of people with little or no practical filament evaluation experience. Twenty-eight microscope phase contrast images of unstained activated sludge samples were selected to represent a broad range of filament contents. Sixteen students assigned FI values to each image using the FI image key provided in Jenkins et al. (2004). Average FI values and standard deviations were based on FI ranking by the 16 participants.

The FI study results were compared to FL/FA values, quantified using both manual tracing and automated image analysis, for each of the 28 microscope images selected for the study. Manual tracing of filament length and floc area was as previously discussed and referred to as FL/FA_M. Automated image analysis was performed using a program written in MATLAB using add-on image processing features (Image Processing Toolbox 3.1: The Mathworks, Inc., Natick, MA). The program included image preprocessing converting color images to binary form, performing a thresholding operation, separating aggregated biomass (floc) from protruding filamentous structures, and debris elimination. Processing involved calculating the lengths of protruding filaments and areas of the flocs which allowed calculation of FL/FA by the automated method, referred to here as FL/FA_A.

8.2.2 Application of Filament Quantification Methods

More than 2800 phase contrast microscope images, generated as part of a study to evaluate seasonal variation of process parameters that effect full-scale wastewater settleability, were quantified by automated (~2000 wet mount images) and manual tracing (~800 hemacytometer images) methods. Approximately 20 phase contrast images (100x) were taken of live, unstained activated sludge samples on a precleaned 25 x 75 mm wet mount slide with a cover slip. These images were used to calculate FL/FA values. A second set of approximately 36 phase contrast images (100x) were taken of live, unstained samples using a hemacytometer slide (Model 3120A Double Neubauer, Hausser Scientific, Horsham, PA). These were used to calculate filament lengths within

a known volume, which when combined with TSS measurements, were used to calculate filament length per dry mass.

Filament quantification of the wet mount images was also performed by the FI ranking (Jenkins et al., 2004) by three individuals for each sample, and automated image analysis methods previously discussed. The automated analysis method was used quantify FL/FA_A for each sample.

Filament quantification of the hemacytometer images was performed by manual tracing as previously discussed. The FL/TSS for a given sample was calculated from the total measured filament length per hemacytometer volume and the sample TSS. The ratio of filament length and floc area was also calculated for the hemacytometer images, referred to here as FL/FA_{MH} .

8.3 Results and Discussion

8.3.1 Filament Index Calibration

FI calibration performed by manual tracing of the FI key images provided by Jenkins et al. (2004) resulted in a significant correlation between filament index and the filament length per floc area ratio (Figure 8.1). Conveniently, the relationship shown in Figure 8.1 indicates that visual FI ranking can be used to approximate filament length/floc area using the following equation:

$$\frac{FL}{FA} = e^{\left(\frac{FI-6.07}{1.12}\right)}$$

The relationship demonstrates that a unit increase in filament content at high values (above FI=5) corresponds to a nearly exponential increase in length per area ratio. The occurrence of filamentous bulking is typically evident at FI > or = 4 (Jenkins et al., 2004) and at high filament content an incremental increase in FI ranking has been demonstrated to correspond linearly with increasing sludge volume index a measure of settleability (Schuler and Jassby, 2007).

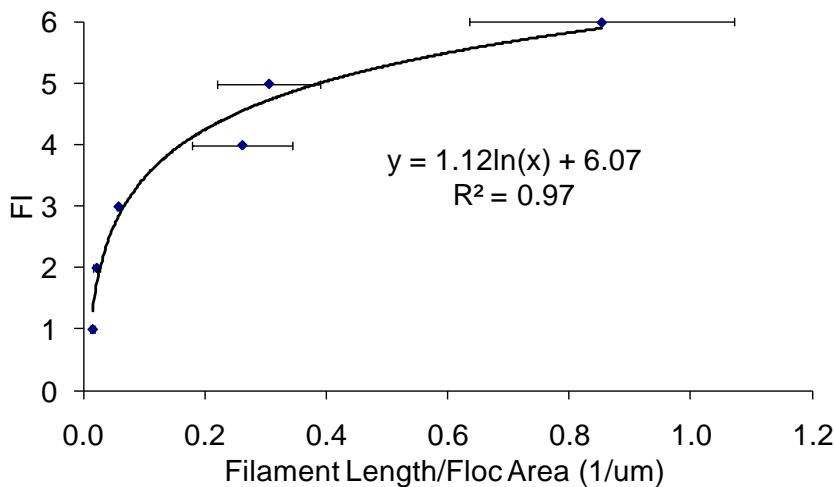


Figure 8.1: The relationship between FI and FL/FA for the Jenkins et al. (2004) FI key images where the FI scale is characterized as 1: few, 2: some, 3: common, 4: very common, 5: abundant, 6: excessive. Error bars represent standard deviations of manual tracing measurements by three individuals.

8.3.2 Filament Index Study

A simple study was conducted to evaluate the relationship between FL/FA and the filament index ranking method to compare automated and manual tracing methods of

quantifying filament length and floc area measurements. The correlation between FI ranking and automated quantification (FL/FA_A) demonstrates a close relationship with the FI calibration (Figure 8.2).

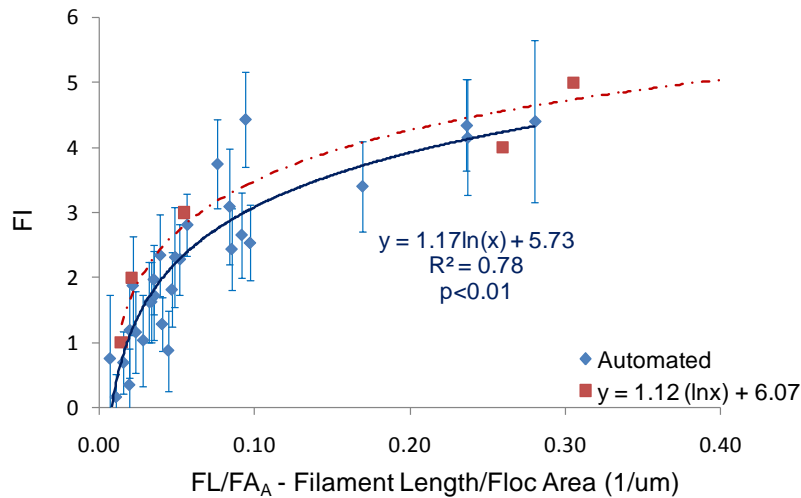


Figure 8.2: Relationship between FI survey results and FL/FA measurements performed using automated image analysis. For comparison, the filament index calibration is included. Error bars represent standard deviations of FI ranking by 16 individuals.

The correlation between FI ranking and manual tracing quantification (FL/FA_M) is strong (Figure 8.3). However, the manual tracing correlation does not correspond as well to the FI calibration compared to the automated method results presented in Figure 8.2.

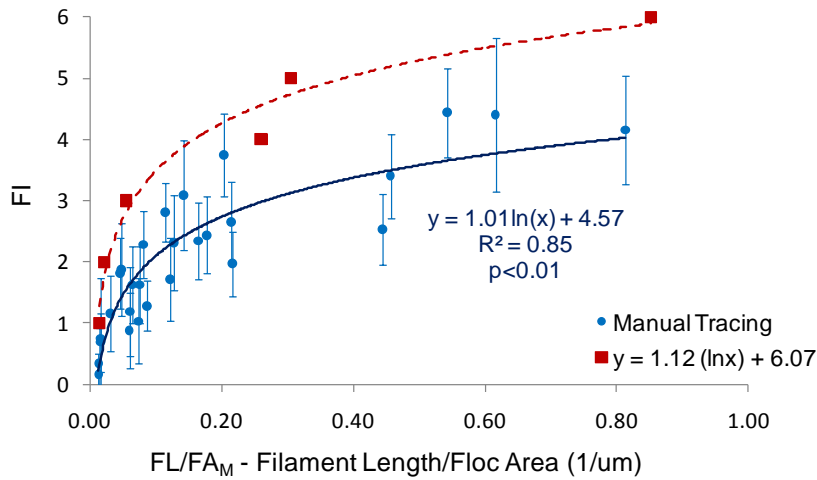


Figure 8.3: Relationship between FI survey results and FL/FA measurements performed from manual tracing analysis. For comparison, the filament index key calibration is included. Error bars represent standard deviations of FI ranking by 16 individuals.

The automated method demonstrated the best agreement with the calibration.

Surprisingly, the automated method of filament analysis gave more similar results to the analysis of the Jenkins et al. (2004) images than did manual tracing (Figures 8.2 and 8.3).

The error bars presented in Figures 8.2 and 8.3 result from the standard deviation of rankings by 16 individuals with little or no filament ranking experience. While these standard deviations are large, the correlation between FI and FL/FA are significant for both automated and manual tracing methods indicating that some portion of the subjective nature of FI ranking can be mitigated by replicate observations.

Comparison of the FL/FA measurements performed by both measurement methods indicates that manual tracing results in a length/area ratio three times that of the

automated method (Figure 8.4). The axes were transformed to logarithmic scales in order to more clearly present the numerous clustered data points at low filament content.

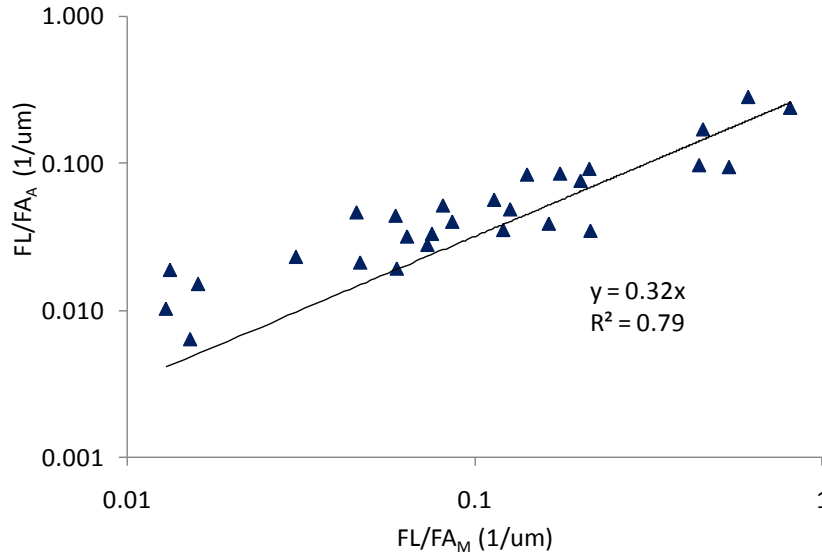


Figure 8.4: Relationship between FL/FA quantified by manual tracing (FL/FA_M) and automated (FL/FA_A) methods for images included in FI survey.

8.3.3 Filament Data for Full Scale Wastewater Plants

Phase contrast microscope images were used to compare filament quantification methods applied to a range of full-scale treatment processes exhibiting a range of filament content. Visual ranking (FI) and automated image analysis (FL/FA_A) methods were used to quantify filament content from wet mount images. Manual tracing was used to quantify FL/TSS and FL/FA_{MH} for images taken using the hemacytometer slide.

Consistent with the FI survey experiment, the correlation between FI ranking and automated FL/FA_A quantification for full-scale wastewater facilities closely agrees (Figure 8.5). Error bars represent standard deviations of FI ranking by 3 individuals and vary by as much as ±0.5 of an FI value. Consistent with the FI survey experiment, the subjectivity of the FI ranking method is mitigated by replicate observations.

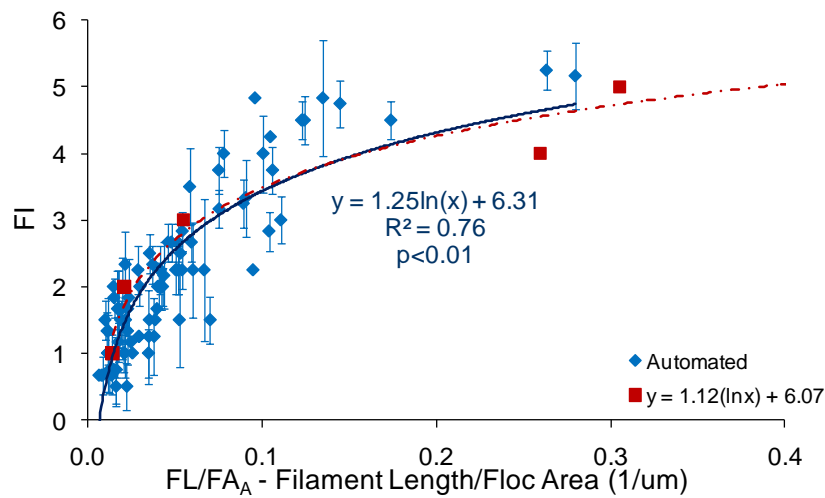


Figure 8.5: Relationship between FI ranking and FL/FA measurements obtained from automated image analysis for full-scale experiment results. For comparison, the filament index key calibration is included. Error bars represent standard deviations of FI ranking by 3 individuals.

The correlation between FI ranking and FL/FA_{MH} quantified by manual tracing (Figure 8.6) does not agree with the FI calibration as closely as does automated quantification method. The relationship between FI and FL/FA_{MH} (Figure 8.6; $y = 1.01 (\ln x) + 5.04$) from the hemacytometer images and the relationship between FI and FL/FA_M (Figure 8.3; $y = 1.01 (\ln x) + 4.57$) from the wet mount images show close agreement even though the images were taken from different slide types.

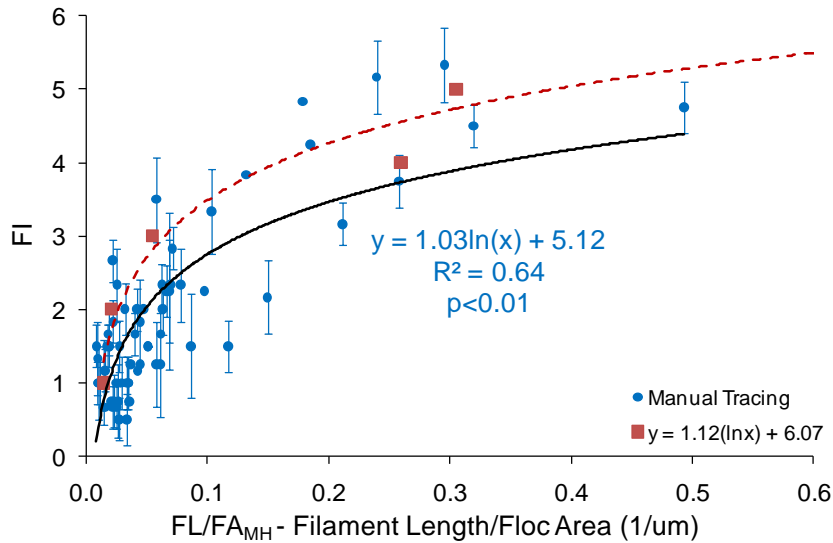


Figure 8.6: Relationship between FI ranking and FL/FA measurements obtained from manual tracing of hemacytometer images for full-scale experiment results. For comparison, the filament index key calibration is included. Error bars represent standard deviations of FI ranking by 3 individuals.

As noted, the highest filament content images evaluated in this study were from MBR facilities which were characterized by pin floc and abundant, short filaments. This apparently tended to produce a lower FI ranking than predicted by the FL/FA ratio. The relationship between the automated and manual tracing quantification methods is included in Figure 8.7. The axes were transformed to logarithmic scales in order to more clearly present the numerous clustered data points at low filament content. The relationship between automated and manual tracing for all data, including the MBR images, indicated a moderate correlation and a 2:1 ratio of the FL/FA_A to FL/FA_{MH} values. When the MBR images are omitted, the correlation substantially improves and the automated results more closely correspond to the manual tracing results (1.25:1 – FL/FA_A to FL/FA_{MH}).

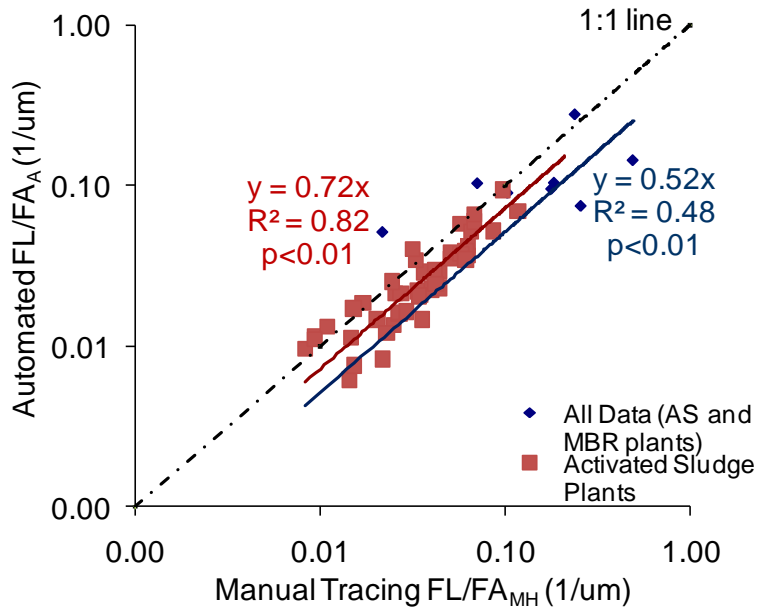


Figure 8.7: Relationship between automated and manual tracing image analysis methods for full-scale experiment results. Correlation improves and approaches a 1:1 relationship when MBR data is omitted.

The relationship between FI ranking and filament length/mass (FL/TSS) from manual tracing of hemacytometer corresponds better with the manual tracing FL/FA_{MH} ratio than with the FI calibration (Figure 8.8).

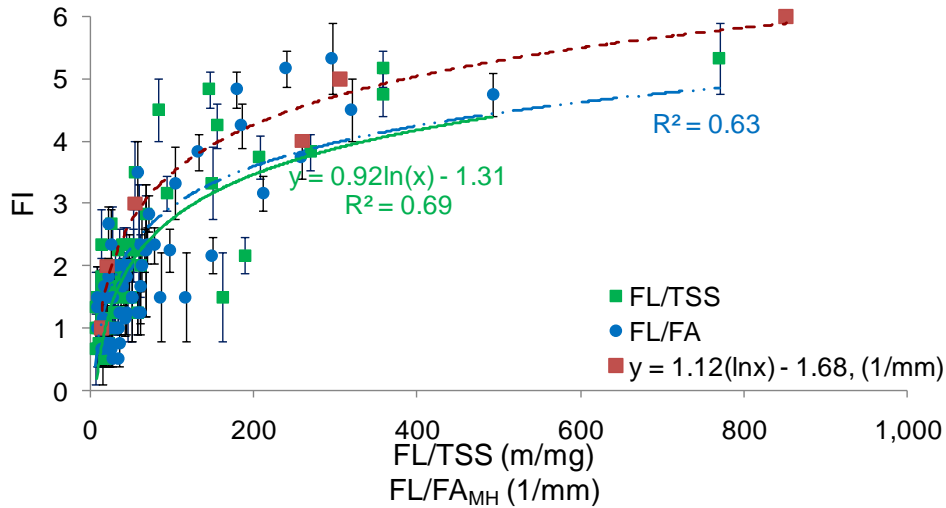


Figure 8.8: Relationship between FI and FL/TSS quantified from hemacytometer images using the manual tracing method. FI calibration and FL/FA_{MH} relationships are repeated here for comparison. The FL/FA units were converted from 1/μm to 1/mm to allow plotting the ratio on the same scale as the FL/TSS measurements.

The primary purpose of performing filament quantification is to develop practices for possible prediction of bulking sludge onset. To that end, filament quantification methods are usually compared with settleability measurements (SVI) to evaluate the predictive ability of the quantification method. Consistent with previous research, filament content by each quantification method was positively correlated with settleability (DSVI). The linear correlation coefficients comparing settleability with filament quantification method is presented in Table 8.1. In this study, the consistency of the correlation between settleability and filament content method indicates that each quantification method had similar predictive capability.

Table 8.1 – Linear regression coefficients relating filament quantification method to settleability as SVI (all correlations are positive)

Filament Quantification Method	R ² (p<0.01)
FI	0.67
FL/FA _A	0.61
FL/FA _{MH}	0.66
FL/TSS	0.63

It is reasonable to expect that both the slide type (wet mount or hemacytometer) as well as the filament measurement methods (automated or manual tracing) affect the filament quantification outcome. From the data presented here, it cannot be determined whether slide type or measurement method had a greater influence on quantification. For example, the relationship between FI and FL/FA for the FI calibration, generated using manual tracing of wet mount images (Jenkins et al., 2004), compared closely with automated image analysis also conducted on wet mount images indicating that slide type was more important than measurement method. In contrast, the manual tracing data generated from hemacytometer images (FL/FA_{MH} and FL/TSS) compared closely with manual tracing of wet mount images used in the FI survey experiment (FL/FA_M), indicating that measurement method had more influence than slide type.

8.4 Conclusions

The FI ranking method has been used for many years and although reliant on visual estimation, it is rapid, simple, and requires minimal equipment. The FI calibration conducted in this study may be useful for relating data sets from different research and/or

for comparing filament data from different wastewater facilities. The qualitative nature of this method can make it difficult to identify subtle changes in filament content and may not be the best method for determining the early onset of bulking conditions. However, when using the FI method performing replicate observations do appear to mitigate some of the subjectivity.

Automated image analysis methods have been suggested to detect subtle changes in filament content making is a promising tool for process monitoring (Banadda et al., 2005, da Motta et al., 2002, Mesquita et al., 2009). Further, automated image analysis can generate a large volume of data with minimal effort, once a robust image analysis code is developed. The major drawback for automated image analysis is the lack of a standardized image analysis method and the need for a digital camera equipment and image acquisition and analysis software.

Use of the hemacytometer slide and manual tracing methods allowed calculation of filament content per dry solids mass thus normalizing the filament content to biomass concentration useful for comparing data from different wastewater sources. Manual tracing is a simple, reliable method for quantifying filament content for relation to solids content; however, the method is very time consuming.

The filament quantification methods compared in this study indicate that no one method is substantially more robust than another and that consideration of available equipment, investigator expertise, and level of effort are each important in selecting the appropriate

quantification method. Currently, there is no single filament quantification method that will apply to all research and/or process monitoring circumstances. As a result, it is useful to understand the advantages and disadvantages of the most commonly used methods so that the maximum quality of data can be obtained for the appropriate level of effort.

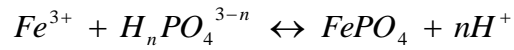
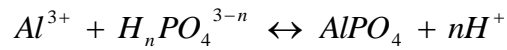
CHAPTER 9

EFFECTS OF PHOSPHORUS CO-PRECIPIATION ON BIOMASS DENSITY AND SETTLEABILITY

9.1 Introduction

The effects of chemical precipitation for removal of phosphorus from wastewater on settleability and biomass density were evaluated. Simultaneous or co-precipitation is the process whereby metal salts are added to a biological treatment reactor to precipitate soluble phosphorus simultaneous with biological treatment, rather than as a separate process. The precipitate phosphorus is then removed during secondary clarification (Bratby, 2006). Co-precipitation is useful for wastewater systems that do not have primary clarification and have limited space to construct tertiary treatment units dedicated to chemical phosphorus removal; however, pH must be monitored closely to ensure that precipitation does not drive the pH so low that biological treatment performance is inhibited (Bratby, 2006).

Phosphorus removal by chemical precipitation can be accomplished through the use of metal ions such as calcium, aluminum, and iron. Only aluminum and iron were used in this study. Important reactions for these precipitants are: (Metcalf and Eddy, 2003):



where n = an integer in the range 0 to 3, depending on the pH.

The actual precipitation mechanisms are considerably more complex, and are dependent on the reaction mixture composition, including competing reactions, alkalinity, pH, trace elements, and ligands (Metcalf and Eddy, 2003). In the absence of competing reactions, the greatest precipitation of aluminum phosphate solid ($AlPO_4$) occurs at pH 6.3 and iron phosphate solid ($FePO_4$) occurs at pH 5.3 (Jenkins and Hermanowicz, 1991). It has been demonstrated that effective phosphorus removal is accomplished at pH close to 7.0, which is characteristic of most biological treatment systems (Jenkins and Hermanowicz, 1991). Design and operation practices that characterize optimum chemical dosing to achieve specific phosphorus removal goals is well established (Bratby, 2006, Metcalf and Eddy, 2003); however, there is limited research into how precipitants influence biomass density and the evidence for how precipitants affect settleability is mixed.

A recent experiment demonstrated a positive correlation between precipitant (ferric chloride) addition and density but improved settling was not observed (Jang, 2006). Both Bratby (2006) and Metcalf and Eddy (2003) indicate that improved settling performance is a positive side effect of co-precipitation using metal salts; however, settling data was not presented. Paris et al. (2005) and Parsons and Berry (2004) report that aluminum salt addition ($AlCl_3$ or Alum) resulted in improved settling performance.

Published data demonstrating degraded settling performance with the addition of aluminum salts was not found. Experimental results addressing iron salt addition and settling varies. Clark et al., 2000 reported that ferric salt addition resulted in consistently higher effluent solids than ferrous salt addition. In contrast, Parsons and Berry (2004) reported that ferrous salts degraded settling more than ferric salt addition. Therefore, clear research evaluating the relationships between chemical precipitation, biomass density, and settleability has yet to be performed

It was hypothesized that formation of metal-phosphate precipitates during co-precipitation would affect density, and that this in turn would affect biomass settleability, which may help explain previous results presented above. The objective of this study was to evaluate these hypotheses in batch experiments of co-precipitation in activated sludge samples.

9.2 *Materials and Methods*

Stock solutions of phosphate (using NaH_2PO_4 at 1 and 2 g/L as P), iron (using FeCl_3 at 2 and 4 g/L as Fe), aluminum (using alum – $\text{Al}_2(\text{SO}_4)_3 \cdot 18\text{H}_2\text{O}$ at 2 and 4 g/L as Al), sodium hydroxide (1 N), calcium chloride (0.5 N) and sulfuric acid (30%) were prepared. A combined stock solution of sodium hydroxide and calcium chloride at a two to one monovalent to divalent (M:D) cation ratio was used for pH correction consistent with research conducted by Novak et al. (1998) in which settling performance was affected by M:D cation ratio. The necessary volumes of activated sludge, stock phosphate solution,

and stock metal solution required to create target metal to phosphorus ratios (presented in Results and Discussion) were calculated using the Goal Seek feature in Excel (Microsoft Corp., Redmond, WA).

9.2.1 Experimental Design

A series of batch experiments were conducted using activated sludge collected from plant AX1 at the beginning of each day of laboratory testing. TSS, VSS, P_{tot} , P_{sol} , biomass density, and DSVI were measured as described in Chapter 4.

The experimental design was made to span the range of accumulated precipitant calculated to occur in a co-precipitation process. Based on a mass balance on an activated sludge system, it can be shown that, assuming 100% precipitation, the accumulated precipitated phosphorus is equal to the influent phosphorus concentration multiplied by the SRT and divided by the hydraulic residence time (HRT). For the purposes of this experiment, it was assumed that an HRT of 0.5 hours and an SRT of 10 days was representative of a typical activated sludge treatment process, resulting in a multiplier (the SRT/HRT value) of 20. The influent phosphorus values evaluated were 2.5 to 5 mg/L, which yielded target precipitated phosphorus values of 50 and 100 mg/L (1.6 to 3.2 mmol/L). A range of metal to phosphorus ratios were evaluated including low (~0.6), medium (~1.2), high (~1.8), and very high (~2.4).

A series of batch experiments were conducted using either ferric chloride or alum as the metal salt. The experiment protocol included starting with 2 L of well mixed activated sludge in a 4L container, placing on a stir plate for continuous mixing, and continuously monitoring pH (Denver Instruments, UB10 probe, Arvada, CO). Following stabilization of the initial pH reading, soluble phosphorus solution was added to the targeted concentrations (range 50 to 100 mg/L). Iron or aluminum salt solution was added to the continuously mixed activated sludge as quickly as pH correction (target between pH 6.0-7.0) could be maintained. Rapid mixing was conducted for five minutes, followed by 20 minutes of slow mixing. Subsequently, sample analyses including TSS, VSS, P_{tot}, P_{sol}, density, and DSVI were conducted.

Table 9.1 – Experimental phosphorus and metal doses

Phosphorus (mg/L)	P (mmol/L)	Metal (as Fe or Al) (mg/L)	Metal (mmol/L)	Metal/P ratio (mmol/mmol)
Ferric Experiments				
44.31	1.43	58.50	1.05	0.73
44.10	1.42	116.67	2.09	1.47
43.66	1.41	169.42	3.03	2.15
43.41	1.40	230.55	4.13	2.95
77.74	2.51	87.72	1.57	0.63
77.00	2.49	186.41	3.34	1.34
76.25	2.46	283.37	5.07	2.06
75.85	2.45	380.37	6.81	2.78
106.66	3.44	122.95	2.20	0.64
105.08	3.39	250.51	4.49	1.32
103.66	3.35	382.93	6.86	2.05
102.19	3.30	519.48	9.30	2.82
Alum Experiments				
42.42	1.37	16.06	0.60	0.43
47.34	1.53	31.12	1.15	0.76
46.67	1.51	52.63	1.95	1.30
46.21	1.49	82.61	3.06	2.05
45.57	1.47	111.59	4.14	2.81
75.55	2.44	43.37	1.61	0.66
74.14	2.39	85.18	3.16	1.32
73.32	2.37	126.48	4.69	1.98

Final concentrations of soluble phosphorus were calculated accounting for background phosphorus present in the activated sludge prior to the experiment and to the concentration of soluble phosphorus added. Actual concentrations of metal salts added were calculated accounting for the volume of base and/or acid added for pH correction (either NaOH/CaCl₂ or H₂SO₄, as needed).

Statistical analyses included univariate linear and non-linear regressions were performed using Excel (Microsoft Corp, Redmond, WA). Correlations were considered statistically significant at a 95% confidence interval ($p < 0.05$).

9.3 Results and Discussion

Phosphorus removal was greater than 90% for both metal coagulants at metal to phosphorus ratios greater than 1.5. Alum addition resulted in better phosphorus removal than ferric chloride at a metal to phosphorus ratio less than one. Figure 9.1 illustrates the phosphorus removal for a range of metal to phosphorus ratios.

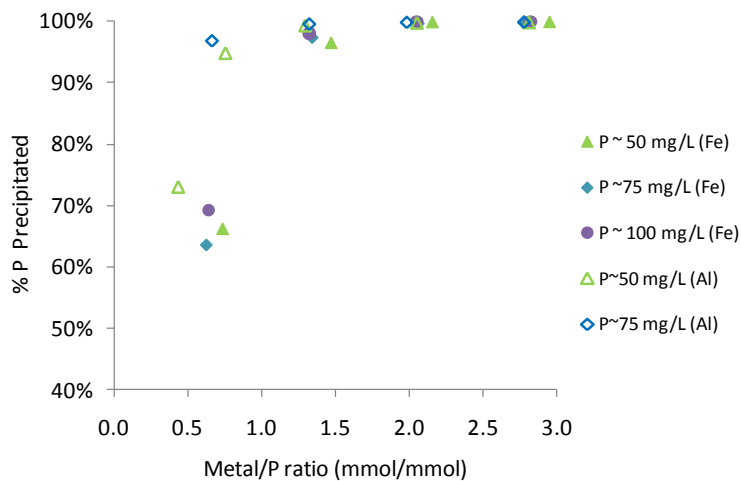


Figure 9.1: Phosphorus removal percentage for all experiments.

9.3.1 Density

Batch experiments demonstrated that metal coagulant addition for phosphorus precipitation significantly increases biomass density according to approximately linear relationships, consistent with Jang (2006). Figure 9.2 illustrates the linear regression of buoyant density and metal dose for both alum and ferric chloride.

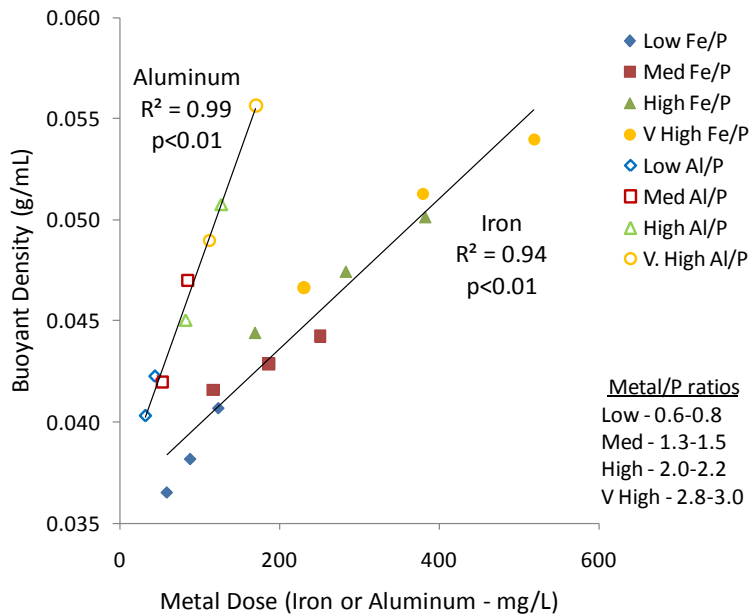


Figure 9.2: Relationship between buoyant density and metal dose for both iron and aluminum for phosphorus doses 50-100 mg/L.

The relationships between NVSS, Pns content, and buoyant density were evaluated. Buoyant density was positively and linearly correlated with Pns/VSS for each metal to phosphorus dosing ratio (Figure 9.3). Pns/VSS includes both biologically stored phosphorus and precipitated phosphorus. The experiments using aluminum salt were conducted for only two phosphorus doses (~50 and ~75 mg/L).

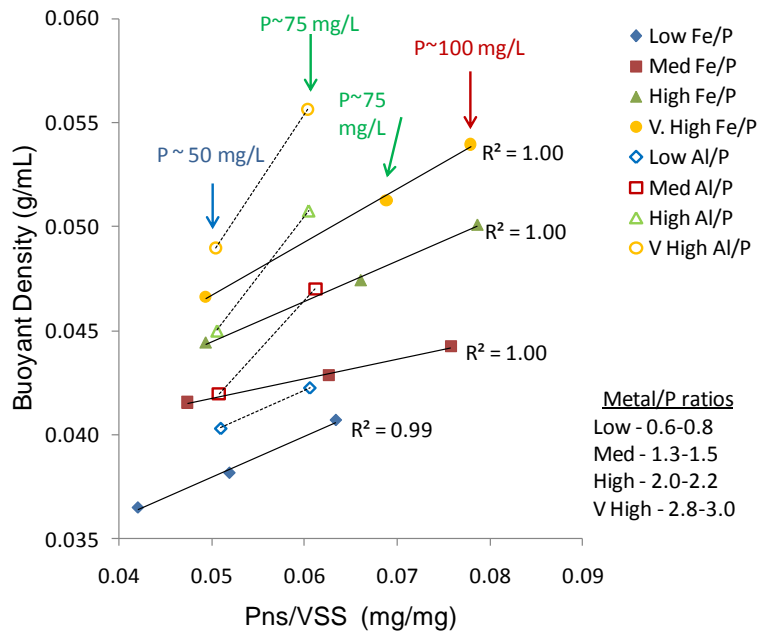


Figure 9.3: Relationship between Pns content (including biomass and precipitated P) and buoyant density. Linear correlations are represented by solid lines for Fe/P and dotted lines for Al/P.

The linear relationships between NVSS and buoyant density were different for iron and aluminum (Figures 9.4 and 9.5). The iron experiments demonstrated different linear NVSS versus density correlations for each metal to phosphorus ratio (Figure 9.4) similar to the linear correlations demonstrated between Pns and density (Figure 9.3). In contrast, the alum experiments demonstrated a NVSS versus density correlation that was linear across the whole data set regardless of metal to phosphorus ratio (Figure 9.5) which is not consistent with the Pns and density illustrated in Figure 9.3. The reason for this dissimilarity between NVSS versus density and Pns/VSS versus density for the alum experiments is unknown.

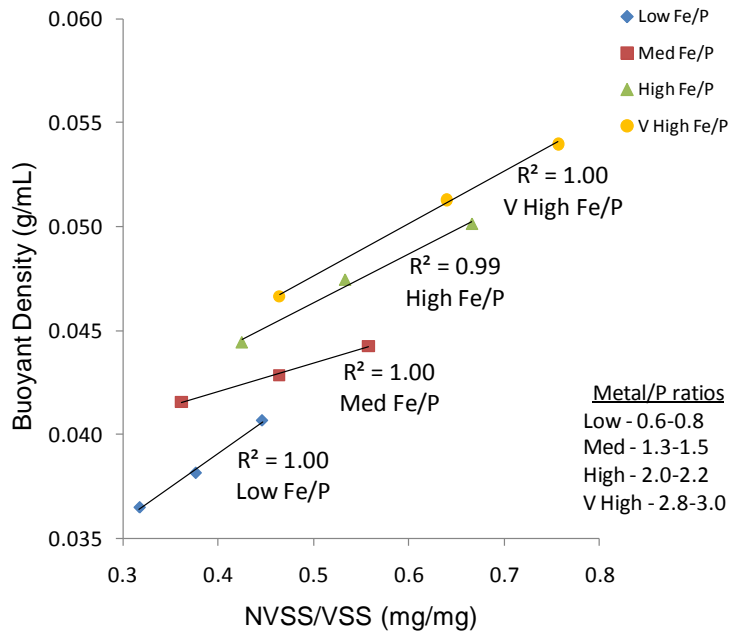


Figure 9.4: Relationship between buoyant density and NVSS content for iron experiments.

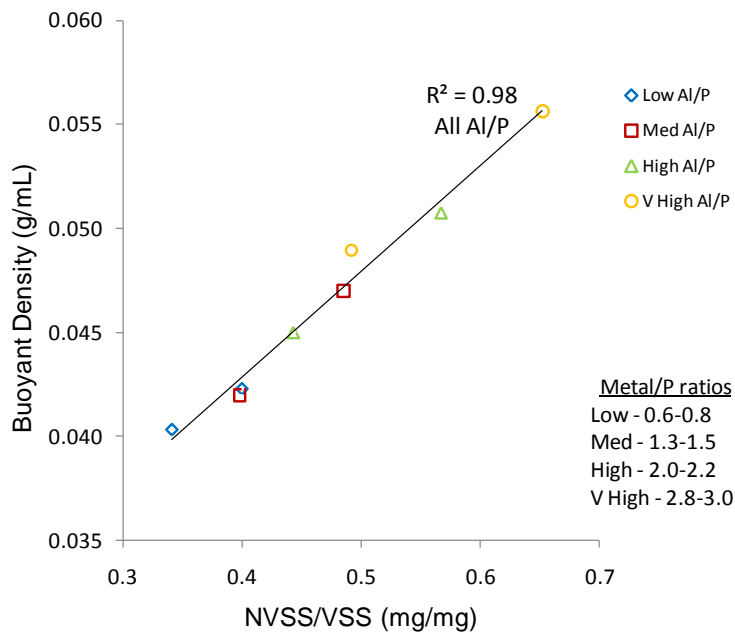


Figure 9.5: Relationship between NVSS content and buoyant for aluminum experiments.

9.3.2 *Settleability*

Previously-presented work in this thesis, and previously published results, have demonstrated that biomass density and settleability are inversely correlated, if other factors such as floc morphology are constant. This experiment tested the hypotheses that phosphorus precipitation affects biomass density, and that this in turn can affect settleability. The results presented above confirmed that precipitate formation increased solids density. However, experiments on settleability yielded the surprising result that settling performance diminished with both iron and aluminum addition (Figures 9.6, 9.8). It should be noted that settleability measured as DSVI was calculated using the total TSS (biomass + precipitant TSS) resulting from each precipitation experiment. The relationships between settleability and metal dose and settleability and buoyant density are discussed separately for iron and aluminum experiments.

9.3.2.1 Iron experiment effects on settleability

Previous research demonstrated that precipitants formed from iron salt addition can negatively impact settling performance (Jang, 2006, consistent with Figure 9.6) with ferric salts causing poorer settling than ferrous salt addition (Clark et al., 2000). The mechanism for this was suggested to be the complexation of iron with organic compounds resulting in large, amorphous floc structures that settle slower and are more resistant to compression in the sludge blanket as compared with biomass floc and/or other metal precipitants (Parsons and Berry, 2004).

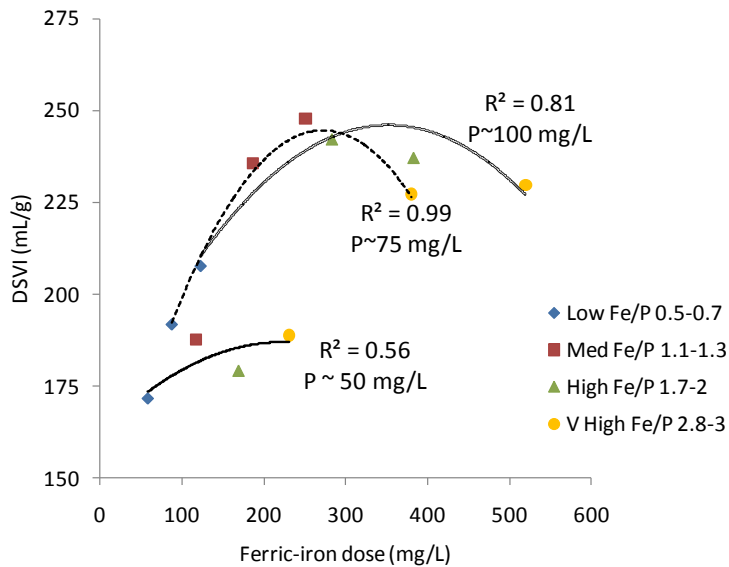


Figure 9.6: Relationship between settleability (DSVI, calculated using biomass + precipitant TSS) and iron dose. Correlations are second order polynomial, and are drawn for each of the three phosphorus doses.

For the iron experiments, settleability degrades most quickly between the low and medium Fe/P ratios which correspond to ~65% and ~95% precipitated phosphorus (Figure 9.1), respectively, for all three phosphorus doses. However, at each phosphorus dose, the high and very high Fe/P ratios, corresponding to greater than 95% precipitated phosphorus, do not appear to further degrade settleability as evidenced by the leveling off (50 mg/L P dose) or improvement (75 and 100 mg/L P dose) in settleability illustrated in Figure 9.6. This parabolic relationship is also evident in the relationship between settleability and buoyant density (Figure 9.7) for the iron experiments and is consistent with other batch experiments (Jang, 2006).

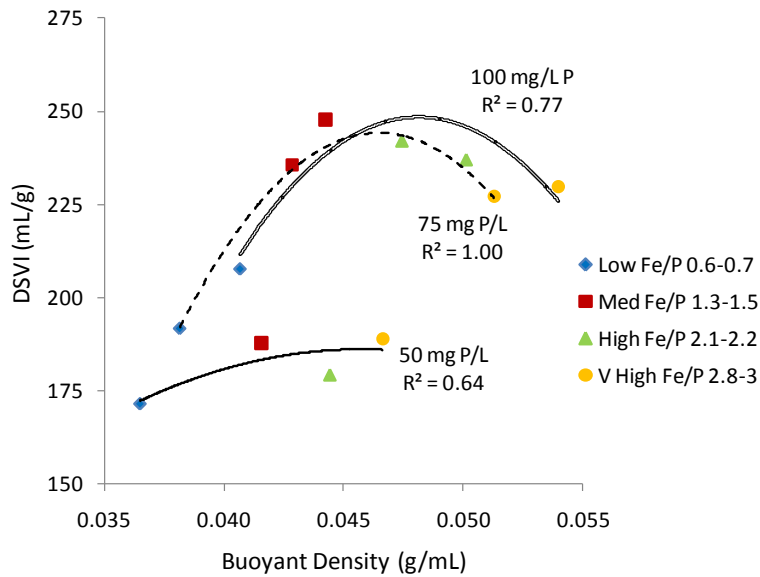


Figure 9.7: Relationship between settleability and buoyant density for iron experiments. Correlations are second order polynomial, and are drawn for each of the three phosphorus doses.

The reason for the leveling off of settleability degradation with ferric chloride addition (Fe/P ratio >1.2) resulting in greater than 95% precipitated phosphorus is not known. It may be possible that large amorphous crystals formed quickly during batch testing initially caused increased drag and resist compression thus degrading settleability. However, the additional phosphorus precipitated above the medium Fe/P ratio continues to increase density and this density increase may help to counteract the drag and compressive resistance imposed by the large floc structures.

9.3.2.2 Aluminum experiment effects on settleability

It has been reported that aluminum salt addition can improve settling performance (Paris et.al., 2005, Parsons and Berry, 2004). However, in this study settling performance

degraded with increasing alum addition (Figure 9.8). It appears that changes to the floc structure, such as those described above for iron addition, due to alum addition more than counteracted any positive influence increased density had on settling. Why this occurred in the current experimental system and not in those of Paris et.al., 2005 and Parsons and Berry, 2004 is not known, but it may have been due to difference in the water quality of the two systems, or in the manner in which the precipitant was added: in full scale systems, the precipitant is added continuously and at a low dose, while in the current study precipitant was added as pulse, which may have led to differences in precipitant structures.

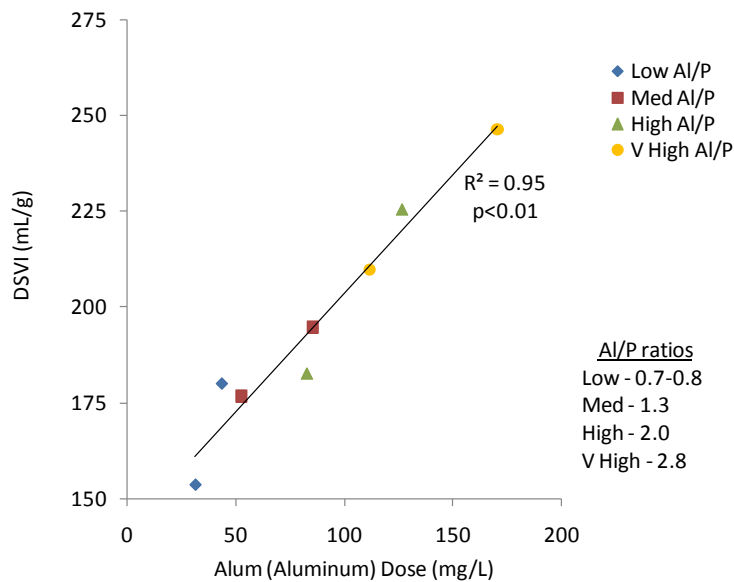


Figure 9.8: Relationship between settleability (DSVI calculated using biomass + precipitant TSS) versus aluminum dose.

In contrast to the iron experiments (Figures 9.6 and 9.7), the aluminum experiments demonstrated linear degradation of settleability for both metal dose and biomass density across all aluminum to phosphorus ratios (Figures 9.8 and 9.9). Settleability continued to

degrade even at greater than 95% phosphorus precipitated indicating that increasing density did not counteract settling degradation in the aluminum experiments. The reason for the difference in settleability relationships between the iron and aluminum experiments is unknown, but adjustment of experimental design (i.e. using continuous metal salt addition to a flow through reactor) may provide a better opportunity to compare precipitant and density effects on settling.

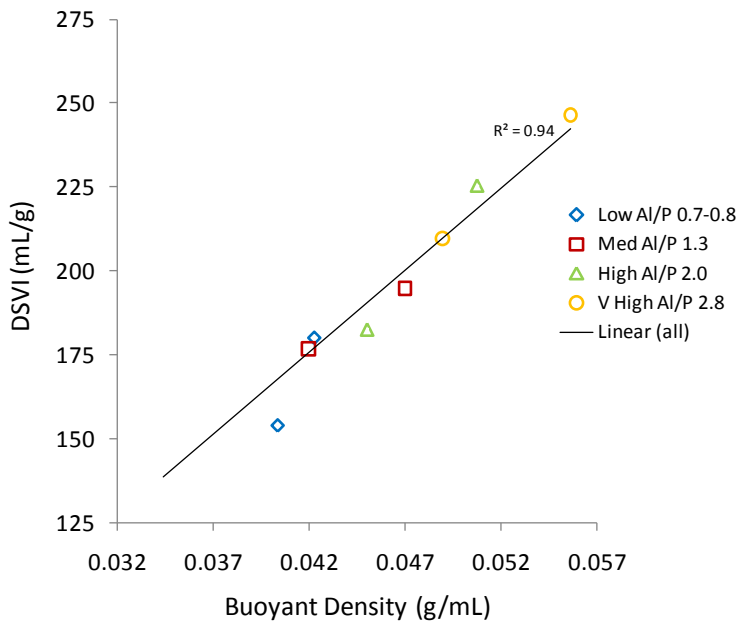


Figure 9.9: Relationship between settleability and buoyant density for alum experiments.

9.4 Conclusions

The results of the precipitation experiment demonstrate that metal precipitants in activated sludge do increase biomass density; however, this particular experiment did not

result a corresponding improvement in settleability. The degraded settling performance resulting from ferric chloride is consistent with previous studies; however, not for the alum experiments. The experimental design used in this study included spiking an activated sludge sample with precipitant, which may have played a role in forming poorly-settling precipitates. A suggestion for future work is to perform this experiment using a lab scale reactor where metal salt dosing is done more slowly to be more representative of full-scale chemical precipitation practices.

CHAPTER 10

CONCLUSIONS

This section summarizes the conclusions presented at the ends of Chapters 5 through 9.

The principal conclusions from the temporal variation studies (Chapters 5 through 7) include:

- 1) Biomass density was significantly higher in warm weather than in cold weather ($p < 0.05$), it exhibited a consistent seasonal cycle that followed ambient and wastewater temperatures in all four full scale activated sludge plants included in this study. None of these trends were evident in two full scale MBR systems.

- 2) Both density and filament content affected settleability. An empirical model of settleability (DSVI) as a function of buoyant density and filament content fit measured data with an R^2 value 0.82. This correlation is notably stronger than modeling settleability as a function of filament content or buoyant density individually. This demonstrates that accounting for both filament content and buoyant density can greatly improve the ability to predict DSVI.

- 3) Biomass density was correlated with NVSS content in all activated sludge plants, consistent with previous work. All of the selector plants exhibited some degree of EBPR, as indicated by elevated phosphorus in the biomass (P_{ns}), and P_{ns} content was correlated with NVSS in the anaerobic selector plant and one of the anoxic selector plants. These

results suggest that seasonal variability in density may be a consistent phenomenon in full scale activated sludge systems, whether or not such systems include selectors. Monitoring of density, along with filament analyses, may help to diagnose the causes of seasonal variations in settleability when they become problematic and may aid in the development of remedial strategies (such as methods to increase NVSS content).

4) While variable settling and phosphorus content was observed during parts of this study, buoyant density consistently remained stable for each sampling events. Daily sampling conducted at plants AX1 and AN indicated that Monday peak phenomena did not occur at these facilities, and so the hypothesis that Monday peaks may lead to temporarily degraded settleability was not tested.

5) Process start-up at plant AN demonstrated variable settling conditions influenced by changes in both biomass density and filament content.

6) A process upset at plant AN caused a degradation of treatment performance with respect to settleability, resulting from significant changes in biomass density and polyphosphate content, without increases in filament content. Process upsets to EBPR systems may therefore result not only in decreased phosphorus removal, but also in degraded settling characteristics linked to loss of polyphosphate from the biomass and consequent decreased biomass density. Polyphosphate and NVSS content have been previously shown to be correlated with biomass density during normal operating conditions of EBPR systems. This study demonstrated that this is true during system

upsets, as well, and so monitoring biomass density may be a useful tool in evaluating overall process performance and upset recovery trends, and differentiating between filamentous growth and biomass density as causative factors in variable settleability.

7) Biomass density measurement is a simple, repeatable test that could be a useful tool in evaluating conditions under both stable and unstable process operation. These results point to practical guidelines resulting from fundamental insights that may provide for improved effluent quality and system performance.

Comparison of filamentous bacteria quantification methods (Chapter 8) yielded the following conclusions:

8) The relationships between three different methods of filament quantification were determined. These may be useful for relating data sets from past and future research and/or for comparing filament data from different wastewater facilities.

9) The filament quantification methods compared in this study indicate that no one method is substantially more robust than another and that consideration of available equipment, investigator expertise, and level of effort are each important in selecting the appropriate quantification method.

The chemical precipitation experiments (Chapter 9) resulted in the following conclusion:

10) The precipitation results demonstrate that metal precipitants in activated sludge do increase biomass density; however, corresponding improvements in settleability were not found, possibility indicating concurrent development of bulking precipitate structures. The degraded settling performance resulting from ferric chloride is consistent with previous studies; but this is not true for previous research on alum addition. The experimental protocol of adding precipitates as a pulse differed from the more gradual accumulation of precipitates during co-precipitation in full scale systems, and may have influenced precipitate characteristics.

CHAPTER 11
APPLICATIONS TO PRACTICE AND
RECOMMENDATIONS FOR FUTURE RESEARCH

11.1 Applications to Practice

11.1.1 Insights to temporal variability of density and settleability at different time scales, and potential for using density measurements for process monitoring

This study demonstrated that biomass density was seasonally variable in four of five full scale activated sludge plants studied, with higher densities in the summer and lower densities in the winter. Biomass density was correlated with non-volatile solids content in each plant, and with non-soluble phosphorus content in some selector equipped plants. Biomass density was also variable during process start-up and upset conditions, and also corresponded with changes in settling at these shorter times scales. The direct density measurement method used in this study is easy to perform and could be a useful process monitoring tool, especially in wastewater systems that are equipped with selectors and/or experiencing upset conditions, and/or in efforts to better understand causes of changes in seasonal settling characteristics.

11.1.2 Filament quantification methods

FI ranking has been used for over 25 years (Eikelboom, 2000) and numerous studies have involved the use of this method to characterize filament content (Andreasen et al., 1996,

Davoli et al., 2002, Krhutkova et al., 2002, Pitt and Jenkins, 1990, Schuler and Jang, 2007a). The method is straightforward and requires a simple microscope. However, the method relies on subjective observations. To the best of our knowledge, this study is the first to determine the relationship between more rigorous filament length measurements (as filament length/floc area and filament length/dry mass) and the FI scale. These relationships may be useful for relating measurements by different methods in previous and future studies.

11.2 Recommendations for Future Research

11.2.1 Factors affecting seasonal density changes should be further evaluated.

This study demonstrated that seasonal biomass density variation is strongly correlated to non-volatile solids content in each activated sludge process and correlated to non-soluble phosphorus content in some of the selector activated sludge plants. Biomass density and non-volatile solids content also correlated with temperature in all plants.

Further research is warranted to explore the factors that cause variable biomass density. For example, research evaluating how and under what conditions temperature, non-volatile solids content, and polyphosphate each effect biomass density would be useful. Results of this research could be useful in refining process operation strategies to improve system performance by optimizing conditions for increased density.

11.2.2 Chemical precipitation effects on density and settling could be further evaluated.

This study demonstrated that metal salts commonly used in chemical precipitation to remove phosphorus increased biomass density; however, a corresponding improvement in settleability was not observed. Previous research by others has indicated that aluminum salt addition improves settling performance at full scale plants (Paris et al., 2005, Parsons and Berry, 2004) and that the settleability performance associated with iron salt addition is mixed (Clark et al., 2000 and Parsons and Berry, 2004). The lack of improved settleability in any samples despite increasing density may be related to the method by which the current batch tests were conducted, with pulse additions of phosphorus and precipitants to activated sludge samples, which may have led to development of large, poorly compacting precipitates. Additional experiments with gradual addition of phosphorus and precipitants, more closely approximating field conditions, may reveal differences in the size/compaction characteristics of the precipitates. The results of this research may provide insight to how and why metal salt addition either improves or degrades settling performance, and why previous studies have found inconsistent results with respect to precipitate effects on settleability.

APPENDIX A
ANALYTICAL PROTOCOLS

Biomass Density

Biomass Density Analysis

Reference: Schuler and Jang, 2007a,b

Equipment:

10 mL culture tubes
1.13 g/mL Percoll solution
Secondary Effluent
Activated Sludge

Procedure:

1. Confirm that secondary effluent, activated sludge, and Percoll solution are all at room temperature (~22° C)
2. Select appropriate range of density solutions for given site, conduct 3 replicates analyses at each density
3. Pipet effluent at specified volume
4. Pipet 1 mL well mixed activated sludge (or other volume as necessary)
5. Pipet Percoll at specified volume, rinse the pipet tip with solution in culture tube to speed Percoll transfer and create well mixed solution
6. Centrifuge samples for 5 minutes at 1000 rpm
7. Visually inspect fraction of biomass on the top of solution for each density and record

DENSITY MEASUREMENT SOLUTION PREP				
density Percoll =		1.13	g/mL	
density sample =		1	g/mL	
Density g/mL	Percoll mL	Effluent mL	Sample mL	Total mL
1.0000	0	1	1	2
1.0033	0.05	0.95	1	2
1.0065	0.1	0.9	1	2
1.0098	0.15	0.85	1	2
1.0130	0.2	0.8	1	2
1.0163	0.25	0.75	1	2
1.0195	0.3	0.7	1	2
1.0228	0.35	0.65	1	2
1.0260	0.4	0.6	1	2
1.0293	0.45	0.55	1	2
1.0325	0.5	0.5	1	2
1.0358	0.55	0.45	1	2
1.0390	0.6	0.4	1	2
1.0423	0.65	0.35	1	2
1.0455	0.7	0.3	1	2
1.0488	0.75	0.25	1	2
1.0520	0.8	0.2	1	2
1.0553	0.85	0.15	1	2
1.0585	0.9	0.1	1	2
1.0618	0.95	0.05	1	2
1.0650	1	0	1	2
1.0683	1.05	0	0.95	2
1.0715	1.1	0	0.9	2
1.0748	1.15	0	0.85	2
1.0780	1.2	0	0.8	2
1.0813	1.25	0	0.75	2
1.0845	1.3	0	0.7	2

Carbohydrate (Phenol Method)

Reference: Dubois et al., 1956.

Equipment:

10 mL culture tubes (clean, disposable)
5% Phenol Solution
Dextrose or Glucose Standard
Concentrated Sulfuric Acid
Spectrophotometer

Procedure:

1. Prepare 5% Phenol solution: **WARNING** – this step requires exceptional care as Phenol is poisonous. Conduct all work with Phenol and acid under the hood. Measure 2.5 grams of phenol in aluminum tray. Place clean 50-100 mL flask on scale, zero, add 40 g DI. Transfer phenol to flask and rinse tray until all phenol is transferred. Add DI to 50 g total solution. Cap and let sit 15 minutes to allow phenol to dissolve, may require shaking to get full dissolution. Keep phenol solution in the dark by wrapping flask in foil.
2. Prepare Dextrose Standards (for 1:10 or greater diluted wastewater, a three point curve using 0 mg/L, 25 mg/L, and 50 mg/L works well). A 500 mg/L stock solution of dextrose is prepared using 0.5 g of dextrose powder in 1L of DI.
3. Digestion:
 - a. Add 2 mL of standard or sample to culture tube
(wastewater is typically diluted at least 1:10 or 0.2 mL in 2 mL)
Working under the hood for the remainder of this step:
 - b. Add 1 mL of 5% phenol
Start Timer:
 - c. Add 5 mL of concentrated sulfuric acid
(do this step slowly but steadily, the solution will boil over the top of the vial if the acid is added too quickly, approximately 15 to 20 seconds to add acid for each vial should be adequate.)
 - d. Allow culture tubes to rest 10 minutes (approximately 18 to 24 tubes can be prepared within the 10 minute timeframe). At 10 minutes, cap each tube and invert 3 times.
 - e. Place tubes in a 25° to 30° C water bath for 10 to 20 minutes before analysis.
4. Analysis:

Measure absorbance at 490 nm.

BIBLIOGRAPHY

- Albertson, O.E. (1987). The control of bulking sludges: From the early innovators to current practice. *Journ. Wat. Poll. Cont. Fed.*, **59**, 172-182.
- Al-Halbouni, D, Traber, J., Lyko, S, Wintgens, T, Melin, T. Tacke, D, Janot, A, Dott, W. Hollender, J. (2007). Correlation of EPS content in activated sludge at different sludge retention times with membrane fouling phenomena. *Wat. Res.*
Doi:10.1016/j.watres.2007.10.026.
- Amaral, A.L., Rodrigues, S., Mota, M., and Ferreira, E.C. (2002). Morphological Characterization of Biomass in Wastewater Treatment using Partial Least Squares. Proceedings of the Second IASTED International Conference, Visualization, Imaging, and Image Processing, September 9-12, 2002, Malaga, Spain.
- Amaral, A.L. and Ferreira, E.C. (2005). Activated sludge monitoring of a wastewater treatment plant using image analysis and partial least squares regression. *Anal. Chim Acta*, 544 (1-2), 246-253.
- American Public Health Association, American Water Works Association, and Water Environment Federation (2005). Standard Methods for the Examination of Water and Wastewater, 21st Edition, Washington D.C.
- Andreadakis, A.D. (1993). Physical and chemical properties of activated sludge floc. *Wat. Res.* **27**, 1707-1714.
- Andreasen, K. and Sigvardsen, L. (1996). Experiences with Sludge Settleability in Different Process Alternatives for Nutrient Removal. *Wat. Sci. Tech.*, **33**, 137-146.
- Banadda, E.N., Smets, I.Y., Jenne, R., Van Impe, J.F. (2005). Predicting the onset of filamentous bulking in biological wastewater treatment systems by exploiting image analysis information. *Bioprocess. Biosyst. Eng.*, **27**, 339-348.
- Bratby, J. (2006). Coagulation and Flocculation in Water and Wastewater Treatment, 2nd Ed.. London: IWA Publishing. Bratby, J. (2006). Coagulation and Flocculation in Water and Wastewater Treatment, 2nd Ed.. London: IWA Publishing.
- Brdjanovic, D., Slanet, A., van Loosdrecht, M.C.M., Hooijmans, C.M., Alaerts, G.J., and Heijnen, J.J. (1998). Impact of excessive aeration on biological phosphorus removal from wastewater. *Wat. Res.*, **32** (1), 200-208.
- Cho, S.H., Colin, F., Sardin, M., and Prost, C. (1993). Settling velocity model of activated sludge. *Wat. Res.*, **27** (7), 1237-1242.

- Chudoba, J. Grau, P. and Ottova, V. (1973). Control of activated-sludge filamentous bulking-II. selection of microorganisms by means of a selector. *Wat. Res.* **7**, 1389-1406.
- Clark, T., Burgess, J.E., Stephenson, I., and Arnold-Smith, A.K. (2000). The influence of iron-based co-precipitants on activated sludge biomass. *Proc. Safety and Env. Prot.*, **78** (B5), 405-410.
- Dammel E.E. and Schroeder, E.D. (1991). Density of activated sludge solids. *Wat. Res.*, **25**, 841-846.
- Da Motta, M., Pons, M.N., and Roche, N. (2002). Study of filamentous bacteria by image analysis and relation with settleability. *Wat. Sci. Tech.*, **46**, 363-369.
- Davoli, D., Mandoni, P., Guglielmi, L., Pergetti, M. and Barilli, S. (2002). Testing the effect of selectors in the control of bulking and foaming in full scale activated sludge-plants. *Wat. Sci. Tech.*, **46**, 495-498.
- Dubois, M., Gilles, K.A., Hamilton, J.K., Rebers, P.A., and Smith, F., (1956). Colorimetric method for determination of sugars and related substances. *Analytical Chem.*, **28**, 350-356.
- Eikelboom, DH (2000). Process Control of Activated Sludge Plants by Microscopic Investigation, 1st Ed., London, IWA Publishing.
- Fainsod, A., Pagilla, K.R., Jenkins, D., Pitt, P.A., and Mamais, D. (1999). The effect of anaerobic selectors on *Nocardia*form organism growth in activated sludge. *Wat. Env. Res.* **71** (6), 1151-1157.
- Gabb, D.M.D., Still, D.A., Ekama G.A., Jenkins, D., and Marais, G.v.R. (1990). The selector effect on filamentous bulking in long sludge age activated sludge systems. *Wat. Sci. Tech.*, **23**, 867-877.
- Graveleau, L., Cotteux, E., and Duchene, P. (2005). Bulking and foaming in France: The 1999-2001 survey. *Acta Hydrochim. Hydrobiol.* **33**, 223-231.
- Henriques, I.D., Kelly III, R.T., and Love, N.G. (2004). Deflocculation effects due to chemical perturbations in sequencing batch reactors. *Wat. Sci. Tech.*, **50**, (10), 287-294.
- Henriques, I.D., Holbrook, R.D., Kelly III, R.T., and Love, N.G. (2005). The impact of floc size on respiration inhibition by soluble toxicants – a comparative investigation. *Wat. Res.*, **39**, 2559-2568.

- Henriques, I.D. and Love, N.G. (2007a). The role of extracellular polymeric substances in toxicity response of activated sludge bacteria to chemical toxins. *Wat. Res.*, **41**, 4177-4185.
- Henriques, I.D., Aga, D.S., Mendes, P., O'Connor, S.K., and Love, N.G. (2007b). Metabolic Footprinting: A New Approach to Identify Physiological Changes in Complex Microbial Communities Upon Exposure to Toxic Chemicals. *Env. Sci. Tech.*, **41**, (11), 3945-3951.
- Jang, H.. Density effects on sedimentation of biological solids for improved wastewater treatment. *Ph.D. thesis*. Department of Civil and Environmental Engineering, Duke University, Durham, North Carolina.
- Jang, H. and Schuler, A.J. (2007). The case for variable density: A new perspective on activated sludge settling. *Wat. Env. Res.*, **79**, 2298-2303.
- Jenkins, D., Richard, M.G., and Daigger, G.T (2004). Manual on the Causes and Control of Activated Sludge Bulking, Foaming, and Other Solids Separation Problems, 3rd Ed.. Boca Raton: Lewis Publishers.
- Jenne, R., Banadda, E.N., Gins, G., Deurinck, J., Smets, I.Y., Geeraerd, A.H., and Van Impe, J.F. (2006). Use of image analysis for sludge characterization: studying the relation between floc shape and sludge settleability. *Wat. Sci. Tech.*, **54**, 167-174.
- Jin, B., Wilen, B-M., Lant, P. (2003). A comprehensive insight into floc characteristics and their impact on compressibility and settleability of activated sludge. *Chem. Eng. Jour.*, **95**, 221-234.
- Krhutkova, O., Ruzickova, I., and Wagner, J. (2002). Microbial evaluation of activated sludge and filamentous population at eight Czeck nutrient removal activated sludge plants during year 2000. *Wat. Sci. Tech.*, **46** (1-2), 471-478.
- Kruit, J., Hulsbeek, J., and Visser, A. (2002). Bulking sludge solved? *Wat. Sci. Tech.*, **46**, 457-464.
- Liao, B.Q., Allen, D.G., Droppo, I.G., Leppard, G.G., and Liss, S.N. (2001). Surface properties of sludge and their role in bioflocculation and settleability. *Wat. Res.*, **35**, 339-350.
- Liao, B.Q., Droppo, I.G., Leppard, G.G., Liss, S.N. (2006). Effect of solids retention time on structure and characteristics of sludge flocs in sequencing batch reactors. *Wat. Res.*, **40**, 2583-2591.
- Lopez, C. and Morgenroth, E. (2003). Modeling the performance of enhanced biological phosphorus removal systems under dynamic loading conditions using different

- mathematical models. *WEFTEC 2003 Conference Proceedings*, Water Environment Federation Conference, Los Angeles, CA, October 2003.
- Love, N.G. and Bott, C.B. (2000). *A Review and Needs Survey of Upset Early Warning Devices*. Water Environment Research Foundation, Report No. 99-WWF-2, Alexandria, VA.
- Love, N.G. and Bott, C.B. (2002). Evaluating the role of microbial stress response mechanisms in causing biological treatment system upset. *Wat. Sci. Tech.*, **46**, (1-2), 11-18.
- Lugowski, A., Patel, J. Nakhla, G., and Ramani, V. (2007). Reduced sludge production in BNR systems: Reality or myth? *WEFTEC 2007 Conference Proceedings*, Water Environment Federation Conference, San Diego, California, October 2007.
- Martins, A.M.P., Pagilla, K., Heijnen, J.J., van Loosdrecht, M.C.M. (2004a). Filamentous bulking sludge – a critical review. *Wat. Res.*, **38**, 793-817.
- Martins, A.M.P., Heijnen, J.J., van Loosdrecht, M.C.M. (2004b). Bulking sludge in biological nutrient removal systems. *Biotech. Bioeng.*, **86**, 125-135.
- Mas, J., Pedros -Alio, C. and Guerrero, R. (1985) Mathematical model for determining the effects of intracytoplasmic inclusions on volume and density of microorganisms. *J. Bacteriol.* 164(2), 749-756.
- Matsui, S. and Yamamoto, R. (1984). The use of a color TV technique for measuring filament length and investigating sludge bulking causes. *Wat. Sci. Tech.*, **16** (10-11), 69-81.
- Means, E. (2004). Water and Wastewater Industry Energy Efficiency: A Research Roadmap. *AWWA RF*, Project #2923.
- Mesquita D.P, Dias, O., Amaral, A.L., and Ferreira, E.C. (2008). Relationship between sludge volume index and biomass structure within activated sludge systems. XVII Congresso Brasileiro de Engenharia Quimica, Recife, September 14-17.
- Mesquita, D.P., Dias, O., Amaral, A.L., and Ferreira, E.C. (2009). Monitoring of activated sludge settling ability through image analysis: validation on full-scale wastewater treatment plants. *Bioprocess Biosyst. Eng.* **32**, 361-367.
- Metcalf and Eddy, Inc. (2003). *Wastewater Engineering: Treatment and Reuse*. 4th Ed., McGraw Hill, New York, NY.
- Middlebrooks, E.J. and Garland, C.F. (1968). Kinetics of Model and Field Extended-Aeration Wastewater Treatment Units. *Jour. Wat. Poll. Cont. Fed.*, **40**, 586-612.

- Mino, T., Arun, V., Yoshiaki, T. and Matsuo, T. (1987) *Advances in Water Pollution Control - Biological Phosphate Removal from Wastewaters*. Ramadori, R. (ed), pp. 27-38, Pergamon Press, Oxford, United Kingdom.
- Noutsopoulos, C., Andreadakis, A., Mamais, P., and Gavalakis, E. (2007). Identification of type and causes of filamentous bulking under Mediterranean conditions. *Env. Tech.*, **28** (1), 115-122.
- Novak, J.T., Love, N.G., Smith, M.L., and Wheeler, E.R. (1998). The effect of cationic salt addition on the settling and dewater properties of an industrial activated sludge. *Wat. Env. Res.* **70** (5), 984-996.
- Palm, J.C., Jenkins, D., and Parker, D.S. (1980). Relationship between organic loading, dissolved-oxygen concentration and sludge settleability in the completely-mixed activated-sludge process. *J. Wat. Poll. Control Fed.*, **52** (10), 2484-2506.
- Paris, S., Lind, G., Lemmer, H., and Wilderer, P.A. (2005). Dosing aluminum chloride to control *Microthrix parvicella*. *Acta Hydrochimica Et Hydrobiologica*, **33** (3), 247-254.
- Parker, D., Appleton, R., Bratby, J., and Melcer, H. (2004). North American performance experience with anoxic and anaerobic selectors for activated sludge bulking control. *Wat. Sci. Tech.*, **50**, 221-228.
- Parsons, S.A. and Berry, T.A. (2004). Chemical Phosphorus Removal. *Phosphorus in Environmental Technology: Principles and Applications*. Valsami-Jones, E. (ed), pp. 261-267, IWA Publishing, London, United Kingdom.
- Pitman, A.R. (1983). Practical experience with biological phosphorus removal plants in Johannesburg. *Wat. Sci. Tech.*, **15**, 233-259.
- Pitt, P.A. and Jenkins, D. (1990). Causes and Control of *Nocardia* in Activated Sludge. *Res. J. Water Pollut. Control Fed.*, **62**, 143.
- Rittmann B.E. and McCarty P.L. (2001) *Environmental Biotechnology*. McGraw-Hill, New York, NY.
- Schuler A.J., Jenkins, D., Ronen, P. (2001). Microbial storage products, biomass density, and settling properties of enhanced biological phosphorus removal activated sludge. *Wat. Sci, Tech.*, **43**, 173-180.
- Schuler, A.J. and Jang, H. (2007a). Causes of variable biomass density and its effects on settleability in full-scale biological wastewater treatment systems. *Environ. Sci. Technol.*, **41**, 1675-1681.

- Schuler, A.J. and Jang, H. (2007b). Density effects on activated sludge zone settling velocities. *Wat. Res.*, **41**, 1814-1822.
- Schuler A.J. and Jassby, D. (2007). Filament content threshold for activated sludge bulking: Artifact or reality? *Wat. Res.*, **41**, 4349-4356.
- Schuler A., Jassby, D., and Xiao, Y. Combined effects of filament length and density on wastewater treatment biomass settling. To be submitted for publication.
- Sears, K., Alleman, J.E., Barnard, J.L., and Oleszkiewicz, J.A. (2006). Density and Activity Characterization of Activated Sludge Flocs. *Journ. Env. Eng.*, **132**, (10), 1235-1242.
- Sezgin, M. Jenkins, D., and Parker, D.S. (1978). A Unified Theory of Filamentous Activated Sludge Bulking. *J. Water Pollut. Control Fed.*, **50**, 362.
- Suresh, N., Warburg, R., Timmerman, M., Wells, J., Coccia, M., Roberts, M.F. and Halvorson, H.O. (1985) New strategies for the isolation of microorganisms responsible for phosphate accumulation. *Water Sci. Technol.* **17**, 99-111.
- Takashima, M. and Yamamoto-Ikemoto (2003). Filamentous bulking control by sponge media in lab-scale SBR process. *Environ. Technol.*, **24** (1), 17-22.
- Tokuz, R.Y. (1991). The Response of Activated Sludge Process to Hazardous Organic Wastes. *Haz. Waste & Haz. Matl.*, **8**, (3), 245-256.
- Vanderhasselt, A., and Verstraete, W. (1999). Short-term effects of additives on sludge sedimentation characteristics. *Wat. Res.*, **33**, 381-390.
- Wilen, B.M., Lumley, D., Mattsson, A., and Mino, T. (2008). Relationship between floc composition and flocculation and settling properties studied at a full scale activated sludge plant. *Wat. Res.*, **42**, 4404-4418.
- Williams, T.; Kelley, C. *gnuplot 4.2*, 2007.